



<https://theses.gla.ac.uk/>

Theses Digitisation:

<https://www.gla.ac.uk/myglasgow/research/enlighten/theses/digitisation/>

This is a digitised version of the original print thesis.

Copyright and moral rights for this work are retained by the author

A copy can be downloaded for personal non-commercial research or study,
without prior permission or charge

This work cannot be reproduced or quoted extensively from without first
obtaining permission in writing from the author

The content must not be changed in any way or sold commercially in any
format or medium without the formal permission of the author

When referring to this work, full bibliographic details including the author,
title, awarding institution and date of the thesis must be given

Enlighten: Theses

<https://theses.gla.ac.uk/>
research-enlighten@glasgow.ac.uk

PHOTOPRODUCTION IN COMPLEX NUCLEI

BY

T. GORDON WALKER

1875

SEPTEMBER 1960.

ProQuest Number: 10656233

All rights reserved

INFORMATION TO ALL USERS

The quality of this reproduction is dependent upon the quality of the copy submitted.

In the unlikely event that the author did not send a complete manuscript and there are missing pages, these will be noted. Also, if material had to be removed, a note will indicate the deletion.



ProQuest 10656233

Published by ProQuest LLC (2017). Copyright of the Dissertation is held by the Author.

All rights reserved.

This work is protected against unauthorized copying under Title 17, United States Code
Microform Edition © ProQuest LLC.

ProQuest LLC.
789 East Eisenhower Parkway
P.O. Box 1346
Ann Arbor, MI 48106 – 1346

PREFACE

This thesis describes the investigations of the author during his period of research, October 1957 to September 1960, in the Department of Natural Philosophy at Glasgow University.

When the author began his research work, studies were being made in the department on the possibility of the "coherent" production of mesons from complex nuclei. The study of the reaction $B^{11}(\gamma, \pi^-)C^{11}$ was initiated by Drs. I.S. Hughes and P.V. March (Proc. Phys. Soc., 1958). The author participated in the accumulation and analysis of the experimental data chapter 2 section 2 and chapter 4 and is solely responsible for the interpretation presented here.

The detection system was rebuilt and extensively modified by the author (chapter 2, section 3) who also developed the chemical separation procedures (chapter 3). Using these, experimental runs were made on (γ, π^-) reactions on S^{34} , Cr^{52} and Ni^{60} (chapter 5). The accumulation of data and evaluation of the cross-sections for these reactions was in collaboration with Dr. March. The interpretation of the results (chapters 6 and 7) is due solely to the

author. The meson reactions constitute the main part of the thesis.

The experimental work involved in the photospallation studies (chapter 9) and emulsion work (appendices A and B) was in collaboration with Dr. W.T. Morton. The interpretation of the results is the author's (chapter 10).

The author would like to express his thanks to Dr. P.V. March for his guidance and assistance during the period of research, to Professor P.I. Dee for his interest and encouragement, and also to the Department of Scientific and Industrial Research for maintenance grants for the three years of research.

CONTENTS

Introduction	1
1. Review of Published Work	3
2. The Detection System	14
2.1 Introduction	
2.2 The initial detection system	
2.3 Modifications and improvements	
3. Chemical Separations	23
3.1 General	
3.2 The separation of Cu^{60} from a nickel target	
3.3 The separation of Mn^{52} from a chromium target	
4. The Reaction $\text{B}^{11} (\gamma, \pi^-) \text{C}^{11}$	32
4.1 Experimental procedure	
4.2 The calculation of the cross section	
4.3 Results	
5. (γ, π^-) Reactions in Sulphur, Chromium and Nickel	41
5.1 The reaction $\text{S}^{34} (\gamma, \pi^-) \text{Cl}^{34}$	
5.2 The reaction $\text{Cr}^{52} (\gamma, \pi^-) \text{Mn}^{52m}$	
5.3 The reaction $\text{Ni}^{60} (\gamma, \pi^-) \text{Cu}^{60}$	
6. The Activity below Threshold	52

I N T R O D U C T I O N

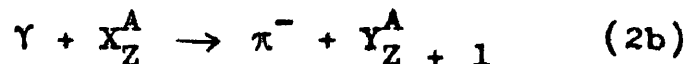
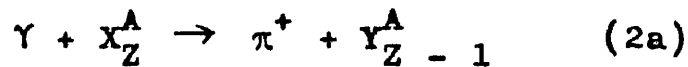
The production of π mesons by the interaction of photons on nucleons i.e. photoproduction of pions, has been studied not only for the purpose of investigating mesons but also to find out more about the nucleons themselves. It is not surprising that most information about the basic photoproduction process can be learned from the production of pions from free nucleons. Such information is useful in determining the properties of the pion field and the character of the pion-nucleon interaction. In general, a study of pion production in complex nuclei reveals information about the behaviour of pions and nucleons in nuclear matter.

Photoproduction processes can be expressed by the following reactions:

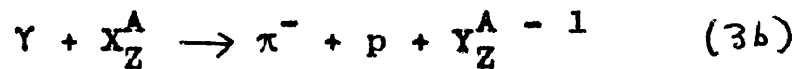
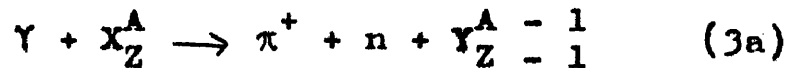
(1) From free nucleons,



(11) From complex nuclei - bound final state,



- continuum final state with single nucleon emitted



where X and Y are the initial and final nuclei, respectively. There are similar reactions for neutral pion production and others involving the emission of several particles.

The reactions investigated in this thesis are those of type (2b), the production of a π^- meson with the struck nucleon remaining in a bound state in the final nucleus.

The basic photoproduction reactions on free nucleons, being two body problems, are quite amenable to calculation. They have been extensively studied both theoretically and experimentally. The photoproduction processes from complex nuclei are more complicated. If, however, pion production is considered as the result of the interaction of a photon with a single nucleon in the nucleus, then comparisons of the reactions from bound and free nucleons will yield information on the effect of nuclear matter on the interacting system.

CHAPTER ONEREVIEW OF PUBLISHED WORK

The earliest experimental work on the photoproduction of charged pions from complex nuclei was performed by Mozeley (1950), Steinberger and Bishop (1950) and Littauer and Walker (1952).

The main features of these experiments were:

(1) The cross-section for the photoproduction of pions from complex nuclei is considerably less than that of the corresponding number of free nucleons.

(2) The sum of the π^+ and π^- meson production cross-sections shows an $A^{2/3}$ dependence, where A is the ~~atomic~~ mass number of the target nucleus.

(3) The ratios of the yields of π^- mesons to π^+ mesons, the π^-/π^+ ratios, show a correlation with the masses of the isobars adjacent in Z, atomic number, to the target nucleus.

Using a Goldberger-Chew momentum distribution for the nucleons in the nucleus and the production cross-section for free nucleons, Lax and Feshbach (1951) derived a value for the π^+ meson production cross-section from carbon. Reasonable agreement with experiment was obtained. However, the π^-/π^+ ratio in carbon could not be explained by

considerations of this type.

Brueckner, Serber and Watson (1951) have interpreted photoproduction on the basis of an optical model taking account of the finite mean free path for the absorption of pions in nuclear matter. According to this model, the production cross-section $\overline{\sigma}_A$ for π^+ mesons from a nucleus of atomic number Z and mass number A can be expressed as

$$\overline{\sigma}_A = \overline{\sigma}_0 \cdot Z \cdot f_a \cdot \eta$$

where $\overline{\sigma}_0$ is the production cross-section from a free proton. η represents the effect of nuclear binding on the cross-section and is not expected to show a uniform trend with A . f_a is a reabsorption coefficient for the pions in the nucleus and is given by

$$f_a = \frac{1}{V_A} \int e^{-\frac{x}{\lambda_a}} d\tau$$

where λ_a is the mean free path for absorption, V is the nuclear volume and x is the path traversed by the meson inside the nucleus. By integration

$$f_a = \frac{3}{4} \frac{\lambda_a}{R} \left[1 - \frac{\lambda_a^2}{2R^2} + \frac{\lambda_a^2}{2R^2} \left(\frac{2R}{\lambda_a} + 1 \right) e^{-\frac{2R}{\lambda_a}} \right]$$

where $R = r_0 A^{1/3}$ is the nuclear radius. From this it may be seen that by taking $\lambda = \frac{A}{2}$ the

relationship $\sigma_A \propto A^{2/3}$ is obtained for $\frac{2R}{\lambda_a} \gg 1$

i.e. when the mean free path for absorption is small in comparison with the nuclear dimensions

For $\frac{2R}{\lambda_a} \ll 1$, $f_a = 1$ and $\sigma_A \propto A$ The value of λ_a is found directly from experiments on the

interaction of pions and nuclei. Littauer and Walker's measurements involved 65 MeV pions for which the mean free path, however, turned out to be of the order of the pion Compton wavelength.

Later, Francis and Watson (1953) indicated that this mean free path could be shown to be compatible with the observed $A^{2/3}$ dependence, in spite of its large value.

Imhof (1957) successfully used the optical model to interpret results over a wide range of pion energies. He considered the effects of the Coulomb potential, the potential arising from the pion nucleon interaction, the internal momentum distribution of the nucleons in the nucleus, and the scattering of pions inside the nucleus. Although his experimental results for pions with varying absorption mean free paths showed an $A^{2/3}$ dependence, Imhof showed, by considering the above corrections,

that there was "fair" agreement between his results and the predictions of the optical model.

A second theory has arisen to explain the experimental results on photoproduction from complex nuclei. In this it is assumed that the formation of real mesons is possible only from nucleons at the nuclear surface. Butler (1952) ^{calculated} ~~determined~~ the production cross-section considering only the surface nucleons, defining surface nucleons as those nucleons which the photon catches beyond the boundary of the main core of the nucleus i.e. with radial coordinates greater than the core radius $R = r_0 A^{1/3}$. The distribution of nuclear density as determined by scattering experiments shows that r_0 , the radius of the core, is about 1.2 fermis. In the surface region the nucleons are subjected only to weak nuclear interactions and may be considered as free. On such a model it was found that the calculated cross-sections displayed an $A^{2/3}$ dependence. This is not surprising since the surface area of a sphere of radius $R = r_0 A^{1/3}$ is proportional to $A^{2/3}$; the volume, of course, is proportional to A . Since the average ratio of protons and neutrons outside the core is dependent on the average binding of neutrons

compared with protons in the nucleus, the trend of the π^-/π^+ ratios with the isobaric mass differences could be satisfactorily explained. However, the calculated values for the production from surface nucleons could account for only 60-70% of the observed pion yields.

The success of Butler's hypothesis indicated that pions are produced preferentially on the surface of the nucleus, pion production being suppressed in the core. Since the observed absorption mean free path appeared too large to account by itself for this suppression, it was explained by a mechanism similar to that proposed by Wilson (1952). According to this a pion produced in the core is immediately reabsorbed by the parent nucleon and another nucleon with which is interacting at that moment. In the case of a free nucleon, and it is assumed that surface nucleons can be treated as such, an intermediate excited state produced by the absorption of a photon has only two modes of decay - either by re-emission of the photon or by the emission of a meson. For a nucleon interacting with a neighbouring nucleon, however, the intermediate state has a third possible mode of decay, namely that in which a meson is

transferred to the ground state of the second nucleon, the excess energy going into the kinetic energy of separation of the two nucleons. Thus the absorption of photons in nuclei may lead, by meson exchange effects between strongly coupled nucleons in the core, to photodisintegration with this latter process having a greater probability than the formation of a real meson. The possibility of observing such processes is indicated in the work of Rosengren and Dudley (1953) who reported the existence of an isotropic component in the angular distribution of photoprotons with an energy close to 70 MeV, which appeared to be due to the absorption of pions by pairs of nucleons. George ⁽¹⁹⁵⁶⁾ also found that his results on the photoproduction of ~~atoms~~^{stars} and mesons in nuclear emulsions supported the Butler-Wilson surface production model.

An evaluation of the two theories of the nuclear core suppression of mesons, the optical model and the surface model, can be made by considering the dependence of the production cross-section on A for slow mesons. For these the mean free path for absorption is long compared with the nuclear radius

and the optical model predicts an A dependence whereas the surface production model gives $A^{2/3}$ independent of meson energy. The relationships can be found in their clearest form in the case of slow π^0 mesons, which is free from Coulomb and Pauli principle effects which complicate the interpretation in the case of charged pions. Belousov et al. (1956) detected π^0 mesons of energies 0 to 30 MeV, for which the mean free path for absorption is about 20%. Except in the region of the lightest nuclei a close fit to an $A^{2/3}$ curve was obtained in agreement with the surface model. Recent measurements by Popova et al. (1959) on the production of π^- mesons of energies 0 to 3 MeV, (for which the nucleus is practically transparent) also confirmed the predictions of the surface production model. The latter results agree with calculations by Baldin and Lebedev (1958) for slow mesons produced from surface nucleons.

The only disagreement of experimental results with the Butler-Wilson model is the 30-40% discrepancy between the magnitudes of the calculated and measured cross-sections. Throughout Butler's calculations it was assumed that the recoiling nucleon had sufficient energy to leave the nucleus.

In the later calculations of Baldin and Lebedev (1958) and Belousov et al. (1959) normalisations were made to carbon, so that quantitative comparisons of the cross-sections cannot be made.

A more detailed calculation on the surface model has been made by Laing and Moorhouse (1957), who considered also the case in which the struck nucleon remains bound in the nucleus. They assumed that the primary photoproduction is essentially a single nucleon process and considered a simple independent particle model for the nucleus in which interparticle forces and spin orbit coupling are neglected. In the primary process the struck nucleon may go into a discrete or a continuum state: this is the only main difference from Butler's treatment, in which only the latter possibility was considered. Laing and Moorhouse pointed out that pion production does not in fact take place as if no other nucleons were present. As well as pion scattering and absorption inside the nucleus these other nucleons will make their presence felt through the operation of the Pauli principle and interparticle forces causing a suppression of pion production from the core. For

their calculations, they considered production from (a) all nucleons and (b) only surface nucleons assuming in both cases that only the outer nucleon shells would contribute and that the s-wave mesons predominated. As an example of a case in which both discrete and continuum states are involved, differential cross-sections and the π^-/π^+ ratio were ~~determined~~^{calculated} for the combined processes,

$$\text{Ca}^{40}(\gamma, \pi^+) \text{X}^{40} \text{ and } \text{Ca}^{40}(\gamma, \pi N) \text{Y}^{39}$$

where π is the charged pion, N the ejected nucleon and X and Y the appropriate residual nuclei. Both surface and volume production values were found. The experimental values of the π^-/π^+ ratios (Hogg and Sinclair, 1956) were closer to the calculated surface production values but the differential cross-sections appeared quite incompatible with the surface production values and about one half of those for volume production. There was, however, some doubt on the absolute values of the cross-sections (Hogg, 1960) due to poor beam calibration at the time of the experimental runs and Hogg and Sinclair's results must be considered as inconclusive.

Laing and Moorhouse have also calculated total

production cross-sections from surface and all nucleons for the reaction $B^{11}(\gamma, \pi^-)C^{11}$, in which the struck nucleon remains bound in the nucleus. The values for volume production are about five times greater than those for surface production. The experimental determination of the cross-section of this process affords a good test for the surface production model.

From kinematic considerations, low incident photon energies imply that any mesons emitted must be slow. Consequently the study of the dependence on ~~atomic~~ mass number of (γ, π^-) processes for photon energies just above pion production threshold will yield a useful comparison of the surface and optical models. Further, since these reactions were not considered in Butler's treatment the cross-sections may be sufficient to remove the discrepancies between Butler's calculations and previous experimental values on the total π^- production cross-sections.

In this thesis measurements are described for the determination of the cross-sections of the reactions $B^{11}(\gamma, \pi^-)C^{11}$ and $Ni^{60}(\gamma, \pi^-)Cu^{60}$.

Attempts to detect similar reactions in elements of intermediate mass are also described. In the case of B^{11} , the experimental values are compared with the calculated values of Laing and Moorhouse. The dependence on A of the B^{11} and Ni^{60} cross-sections is compared with the predictions of the surface production and optical models. Finally the absolute values are compared with Butler's calculated and Littauer and Walker's experimental values.

CHAPTER TWOTHE DETECTION SYSTEM2.1 Introduction.

In general, total cross-sections for the photoproduction of pions have been evaluated from differential measurements by extrapolating to angles at which no measurements were made and integrating over all angles. All previous experiments have depended upon the detection of the pions in certain fixed energy and angular intervals. The complex counter systems generally used make no distinction between reactions in which the meson is accompanied by the emission of other particles and reactions in which the meson is the only particle emitted.

Photopion emission from a complex nucleus, unaccompanied by other particles results in the formation of a nucleus of the same mass as the struck nucleus, and with one charge less, the same charge or one charge greater than, the initial nucleus, according to the charge of the emitted pion. Only charged meson production can result in a radioactive final nucleus. If these nuclei are β -emitters the production cross-sections can be found by measuring the β -activity of these nuclei. The (γ, π^-) type of reaction can be studied more readily than the (γ, π^+) reaction because

the residual nucleus in the former is generally a positron emitter and advantage can be taken of the annihilation quanta to use coincidence counting and so eliminate much of the background counting rate. This method is preferable to counting the positrons directly since it allows the use of thick samples. Another advantage of studying the (γ, π^-) reaction is that the only other method of production of the residual nucleus is by reactions of the type $X_A^Z(p,n)Y_A^Z + 1$ or $X_A^Z(d,2n)Y_A^Z + 1$ etc. and it is possible to detect and remove the charged particle contamination of a bremsstrahlung beam. On the other hand, the residual nucleus of the (γ, π^+) reaction can be produced by the reaction $X_A^Z(n,p)Y_A^Z - 1$ and the neutron contamination is difficult to detect and reduce. Thus the present work has been confined to the investigation of the reaction $X_A^Z(\gamma, \pi^-)Y_A^Z + 1$, the positron activity of the nucleus Y being measured by detecting the annihilation quanta in coincidence.

2.2 The Initial Detection System

Positrons at rest are annihilated by uniting with a free or loosely bound electron, their entire energy appearing in the form of two quanta of equal

FIGURE 2.1

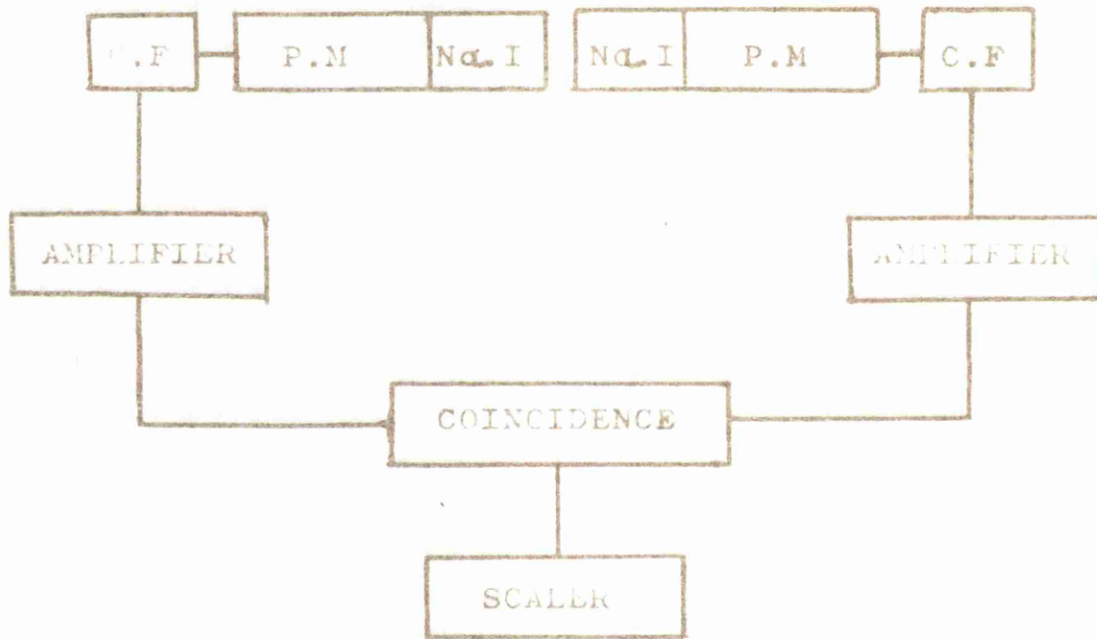


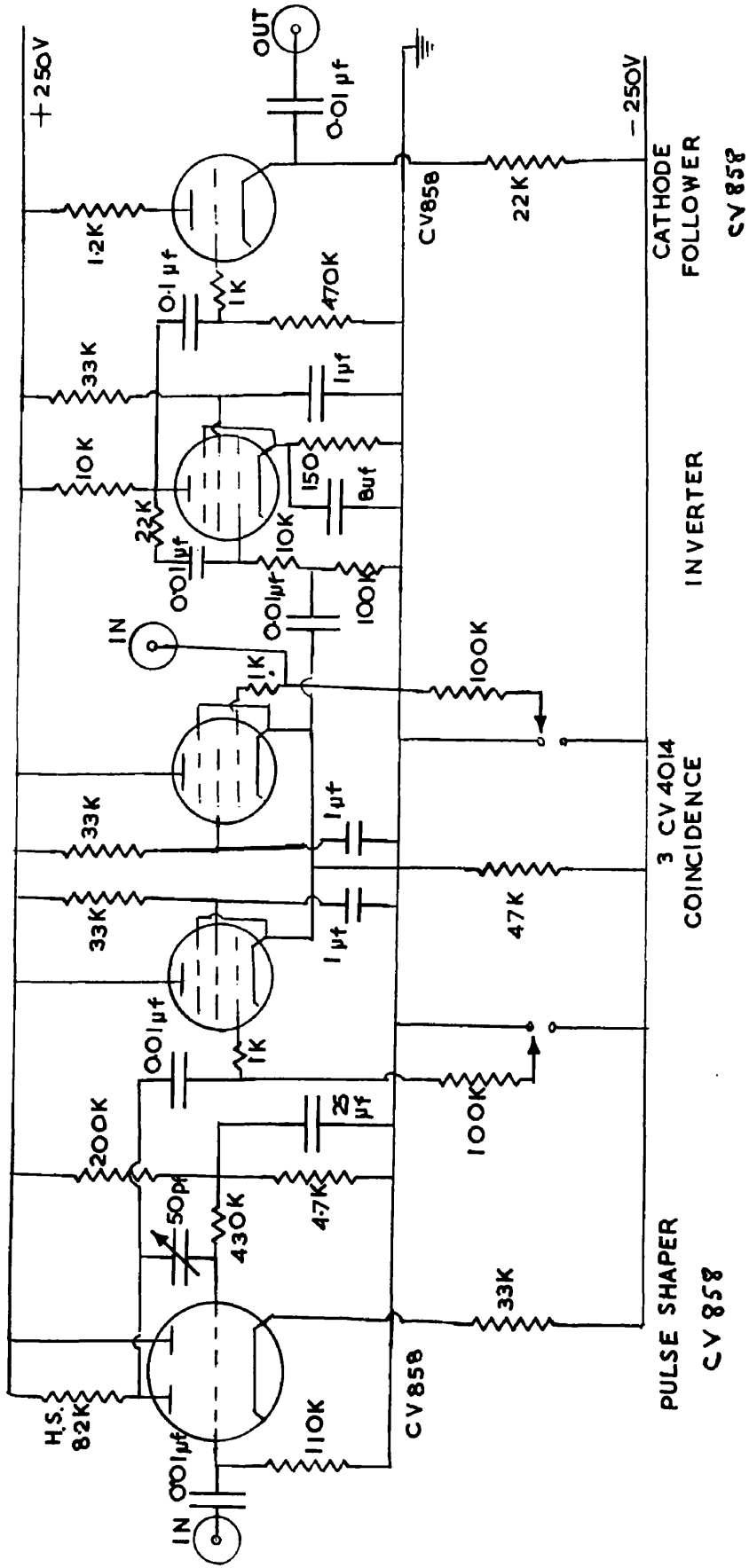
Fig. 2.1: The Basic Detection System
(P.M.; Photomultiplier. C.F.; Cathode follower)

energy (0.51 MeV) emitted in opposite directions. Two low energy γ -ray counters in coincidence at 180° will then serve as a positron detector.

The 0.51 MeV quanta are detected by two $1\frac{1}{2}$ in. x 2 in. sodium iodide (thallium activated) crystal scintillators mounted on E.M.I. 6262 photomultipliers. NaI(Tl) crystals have a high efficiency for the detection of photons since the high atomic number aids photon absorption. The amplified pulses from one photomultiplier are used to gate the amplified pulses from the other, and the coincident pulses are counted on a scaler. A block diagram of the detection system is shown in figure 2.1. The circuit of the proportional-output coincidence unit is given in figure 2.2.

The length of the signal pulses is less than 1 microsecond ($1 \mu\text{s}$) and the gate length of the coincidence unit is $4 \mu\text{s}$. The resolving time of the unit would, therefore, be expected to be $4 + 1 = 5 \mu\text{s}$. This was confirmed using two independent sources as follows. The ~~two~~ counters were separated so that only random coincidences N_R would be recorded. The numbers of pulses registered in unit time by ~~the two~~ counters,

FIGURE 2.2



PROPORTIONAL OUTPUT COINCIDENCE UNIT.

N_1 and N_2 were used to determine the resolving time from the relation

$$N_R = 2 \tau N_1 N_2$$

The resolving time was found to be 4.5 μ s in good agreement with the expected value.

The photomultiplier voltages were set such that any slight voltage drift would have minimum effect on the recorded counting rate. Only those pulses corresponding to the photoelectric absorption of the 0.51 MeV quanta were selected for counting. The correct scalar setting was obtained by varying the discriminator voltage until it corresponded to the minimum which separates the pulses due to Compton scattering from those due to photo-electric absorption. A kicksorter spectrum of the coincidence pulses from a positron source is shown in figure 2.3. The counting rate as a function of the scalar discriminator setting is also shown. The pulses selected for counting are those to the right of the arrows. Throughout synchrotron runs the stability of the electronics was regularly checked by observing the positron emission of a Na^{22} source (half-life-2.6 years).

The detection system in this form was used in the

FIGURE 2.3

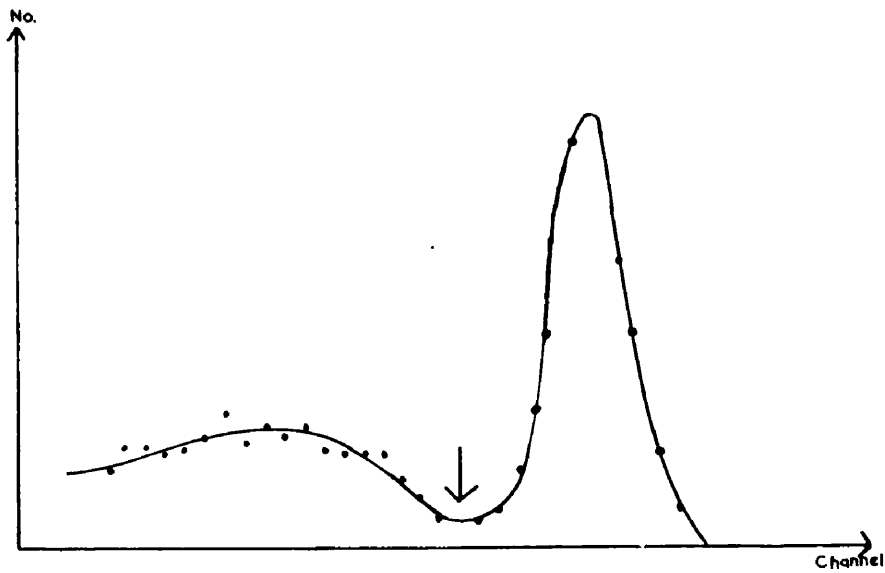


Fig. 2.3(a) Kicksorter spectrum of a C^{11} positron source. The pulses to the left of the arrow are those due to the photo-electric absorption of the 0.51 MeV annihilation quanta.

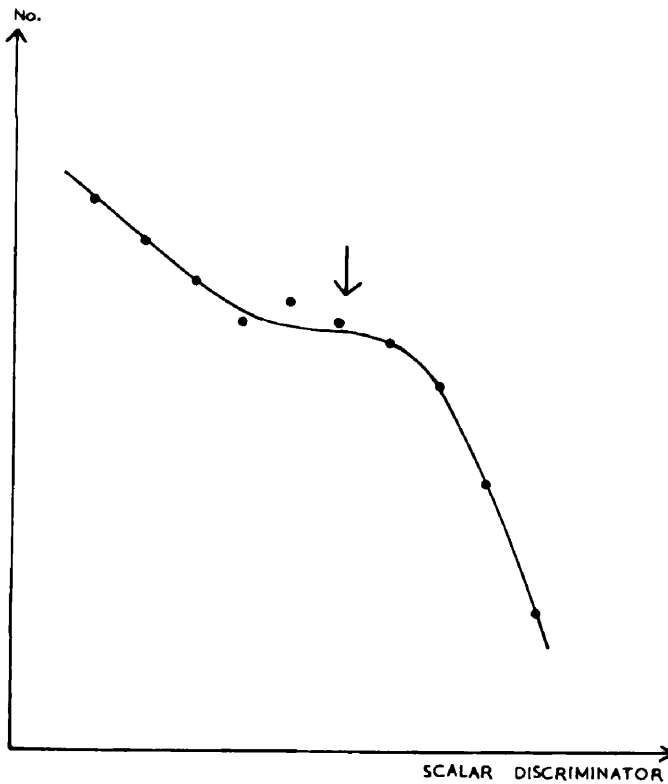


Fig. 2.3(b) Scalar reading as a function of discriminator voltage for the C^{11} source.

measurements on the (γ, π^-) reactions on B^{11} and S^{34} . Slightly modified and to a large extent rebuilt, it was also used for the photospallation measurements.

2.3 Modifications and Improvements.

In order to extend the (γ, π^-) measurements to elements of higher A, it became necessary, particularly at low bremsstrahlung energies, to measure counting rates comparable with the background rates of this detection system. Consequently several means of reducing background were attempted.

It was found that the background was reduced by 40% if the counters were completely enclosed by four inches of lead. A rapid removal and replacement of several heavy lead blocks is, however, necessary to interchange sources with the minimum loss of sample activity. To allow access for sample changing, to prevent damage to or instability in the electronic equipment, lead blocks were placed only at the sides of the counters. This effected an 8% reduction in the background counting rate.

Many background coincident pulses are the result of cosmic ray showers. Two secondaries arising from the same primary and detected in separate crystals will

FIGURE 2.4

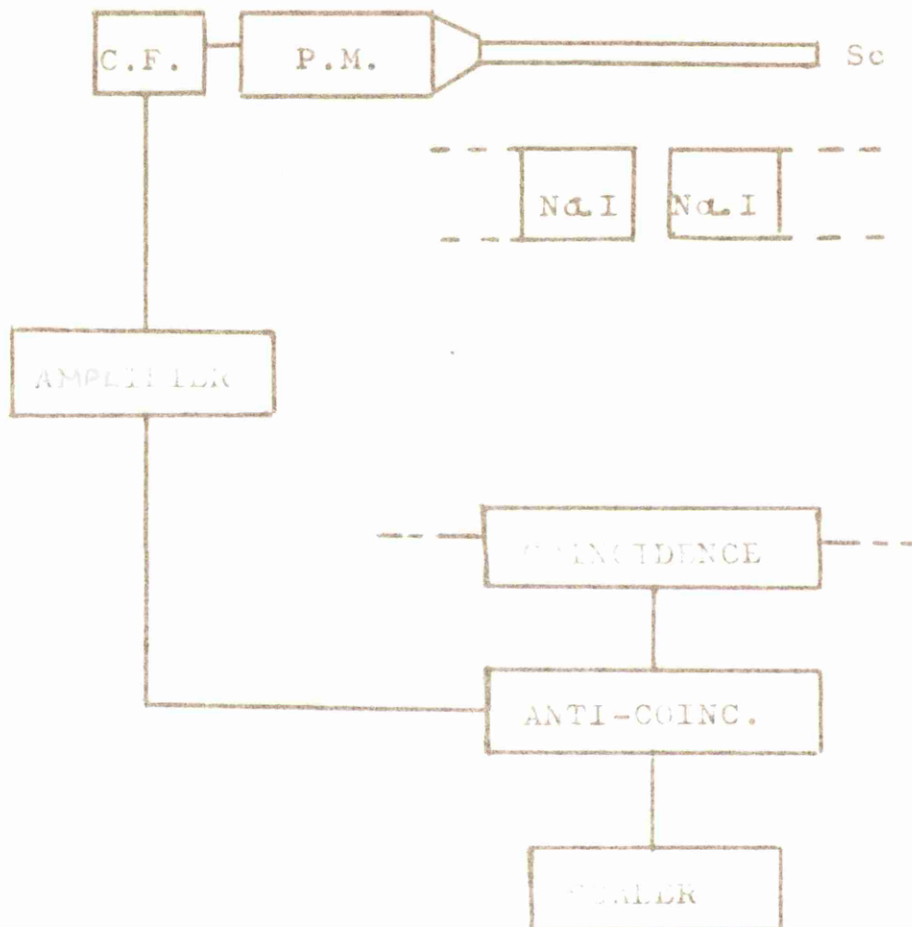


Fig. 2.4: The Anti-coincidence Shield
(Sc: plastic scintillator. P.M. & C.F. as before.)

be coincident in time. To eliminate the effect of these a six inch diameter plastic scintillator was placed above the crystals to act as an anticoincidence shield. Background coincident pulses from the NaI crystals and in anticoincidence with the plastic scintillator pulses were recorded. The additional equipment for the anticoincidence shield is shown in block diagram from in figure 2.4. It was found that this method was successful in making a significant reduction in the background counting rate. On comparing the spectrum of coincident background pulses with that from a positron source, it was observed that only 45% of the background pulses normally counted were in the region of the photo-electric peak for 0.51 MeV quanta. It was further noted that the pulses removed by the anticoincidence shield were beyond the region of the peak. Consequently the anticoincidence shield was discarded in favour of a pulse amplitude selector.

A multi-channel kicksorter is not suitable for rapid quantitative activation measurements due to the time required to record the data. To select pulses due to the photo-electric absorption of 0.51 MeV

FIGURE 2.5

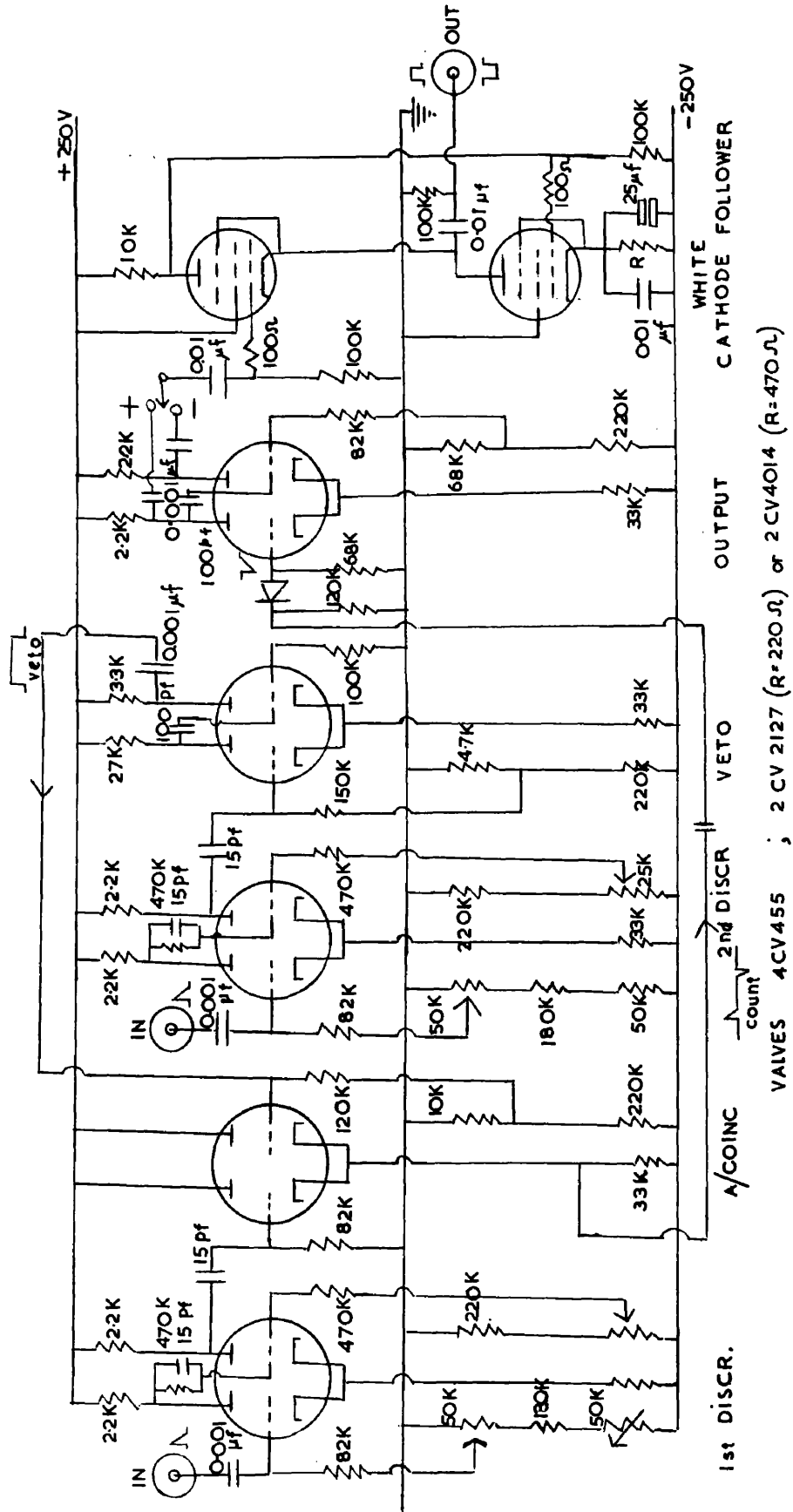


Fig. 2.5 : THE PULSE SELECTOR.

quanta, a single channel pulse height analyser was constructed. In this selector the two threshold voltages were defined by Schmitt trigger circuits. A standard output pulse is generated when the input exceeds the lower threshold but not the upper, and vetoed by an anticoincidence circuit when both thresholds are exceeded. No pulse is generated when the input is below both thresholds. The input pulse was taken from the coincidence output from the positron detection system, and the output fed into a scaler. The circuit diagram is shown in figure 2.5. Since there is pulse discrimination at two levels, voltage drift or instability would have a two-fold effect on the counting rate. In addition, therefore, the pulse selector output was used to gate the input pulses and the resultant coincident pulses displayed on a 100 channel kicksorter. [The circuit of the coincidence unit used appears in figure 2.6.] In this way a continuous check can be made on the discriminator levels. With the original detection system, the setting of the discriminator level could not be done accurately in less than 30 minutes

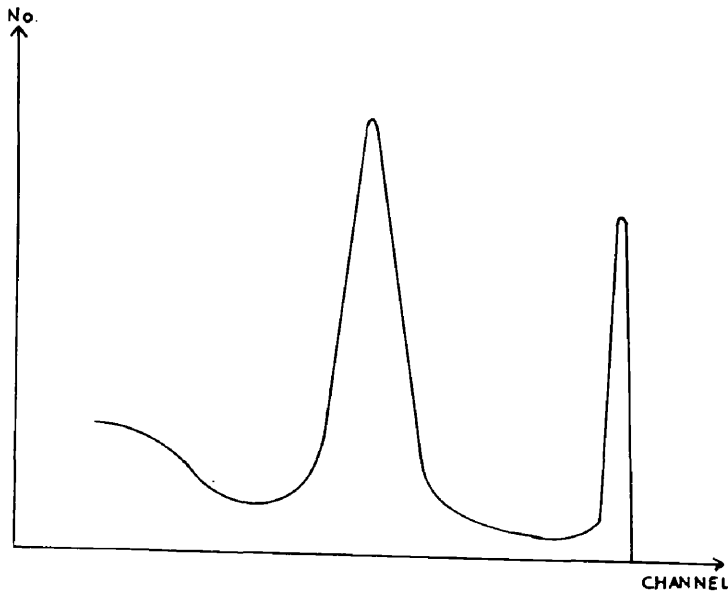


Fig. 2.7. Spectrum of pulses from a Na^{22} source. The large peak is due to the 0.51 MeV annihilation quanta. The other peak is caused by the saturation of the 1.3 MeV γ -ray pulses.

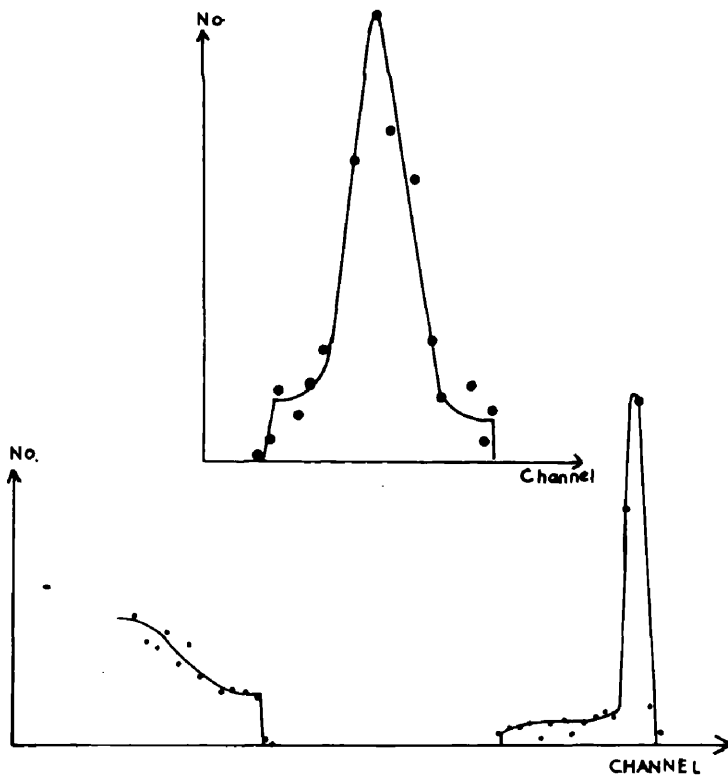


Fig. 2.8 (upper). The pulses selected for counting as displayed on the kicksorter.

Fig. 2.8 (lower). The remaining pulses.

and so the number of checks and resettings made each day was limited. In the present system, any alteration in the pulse height of the 0.51 MeV pulses or in the discriminator levels can be immediately observed and rectified. It is thought that most alterations in the pulse heights was due to mains surges. These are particularly noticeable when the synchrotron power is switched off at the end of a day's running. After an initial warming-up period the equipment generally remained stable throughout the day. In figure 2.7 the spectrum of pulses from a Na^{22} positron source is shown. The pulses which appear beyond the 0.51 MeV photoelectric peak are due to the 1.3 MeV γ -ray in the decay scheme. Of these pulses the ones selected for counting in the scaler are shown in figure 2.8 (a) and those rejected are shown in figure 2.8 (b).

A block diagram of the final modified detection system is shown in figure 2.9. This system was used for the $\text{Cr}^{52}(\gamma, \pi^-)\text{Mn}^{52}$ and $\text{Ni}^{60}(\gamma, \pi^-)\text{Cu}^{60}$ measurements. Using the original detection system, the

FIGURE 2.9

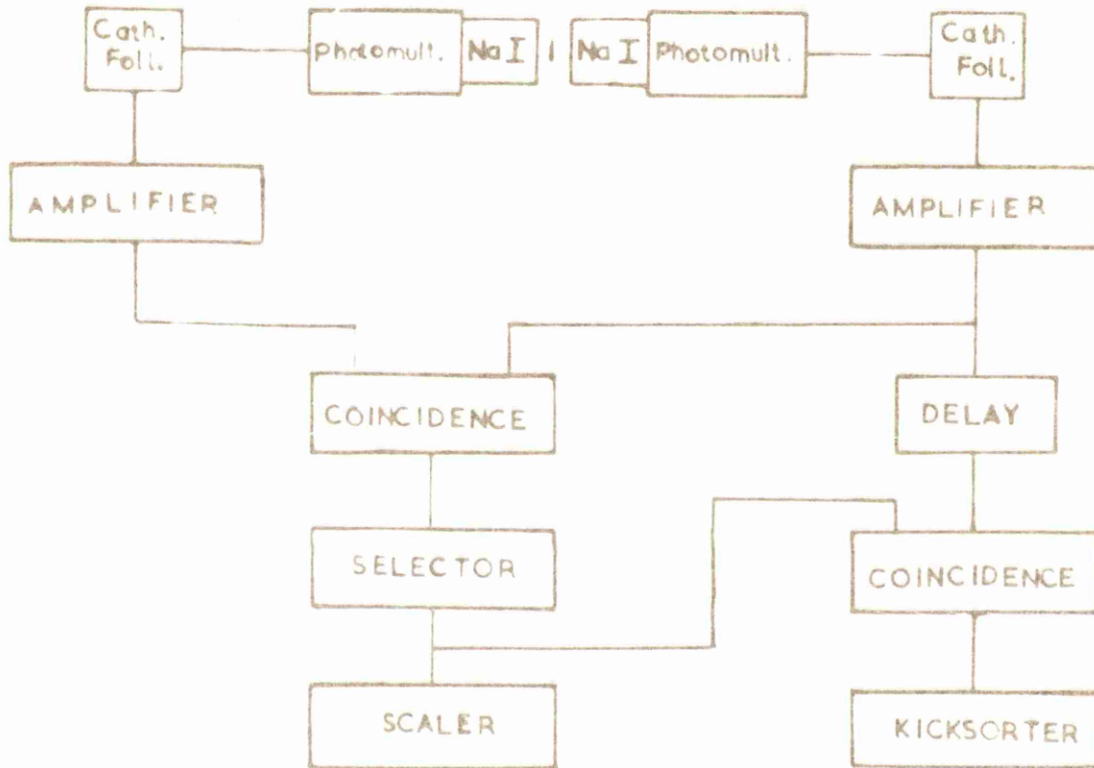


Fig. 2.9 The Final Detection System

counting rate due to background was 14 counts per minute. The background counting rate for the new system is 6 counts per minute, a decrease of 57%. A further advantage of this system is that it can readily be maintained stable throughout the long synchrotron runs.

CHAPTER THREECHEMICAL SEPARATIONS.3.1 General.

By the exposure of a one gram target to a high energy particle or photon beam, there will be produced in it a large number of radioactive isotopes. In order to isolate one particular element it is necessary to separate an element whose total mass may be of the order of 10^{-12} g. from several other elements present in similar quantities in the 1 g. target mass. Such a separation is necessarily different from standard chemical procedures.

The principle upon which radiochemical analysis is based is that if a precisely determined quantity of an element is added to a system containing radioactive isotopes of the same element and if complete exchange is attained (e.g. as occurs in a solution), the radio-isotope is chemically inseparable from that added to the system. Of course, as far as activity measurements are concerned only the active portion can be detected. Any fractional loss of the radio-isotope can be measured by the fractional loss in the added element. The term carrier is applied to

this element for obvious reasons. Hold-back carriers of elements of the undesired active isotopes are also added to the system to retain these isotopes in the system when the element under investigation is extracted. So by a combination of physical and chemical techniques the quantity of a particular radio-isotope present in the original system can be determined.

In general radiochemical studies have involved the irradiation of target foils, the addition of milligram quantities of carrier elements to a solution of the target, and the subsequent application of modified micro or semimicro chemical separation to obtain the required separated fractions. These were then mounted on thin counting trays and exposed to shielded Geiger or proportional counters. The experimental procedure adopted for the present measurements entails the use of thick samples. The radiochemical procedures developed for 100 mg. targets may not be those applicable for 10 g. targets. Using macro quantities of separation chemicals, filtering, adsorption and co-precipitation present greater

problems than encountered in standard radiochemical separations. In the development of the separation techniques described in this chapter, a trial and error method of determining the best separation based on the standard separations of radiochemical and macro quantitative analysis was adopted.

3.2 The Separation of Cu^{60} from a Nickel Target

The nickel used was Mond Nickel Powder, grade A, the impurities being: oxygen 0.1%, carbon 0.05 - 0.1%, iron 0.01% and sulphur 0.001%. Since there are no impurities of Z greater than that of nickel, copper can be produced in a photon beam only by a reaction of the type $\text{Ni}(\gamma, \pi^-)\text{Cu}$. An examination of the periodic table (figure 3.1) shows that the isotopes, with activities similar to Cu^{60} , most likely to be produced from nickel are Ni^{57} , Co^{55} , Fe^{52} , Mn^{52} , Mn^{51} , Cr^{49} , V^{47} , Ti^{45} , Sc^{44} , Sc^{43} and K^{38} . Owing to the small cross-section of (γ, π^-) reactions any chemical extraction of Cu must also leave behind these interfering elements. The only interfering nuclide produced from the nickel impurities will be C^{11} , which can be produced by a (γ, n) reaction on C^{12} or a

($\gamma, \alpha n$) reaction on O^{16} . A comparison of (γ, π^-) and (γ, n) cross-sections shows that the carbon activity must be almost completely eliminated from the separated copper. A further necessity of the separation is that it must be performed in a time not much greater than the half-life of Cu^{60} i.e. 24 minutes. The required separation then is of copper from a nickel sample in the presence of cobalt, iron, manganese, chromium, vanadium, titanium, scandium, potassium and carbon. The separation must also be rapid and efficient, so that the Cu^{60} activity will be measurable.

After irradiation the nickel sample (of mass 10 g.) was dissolved in aqua regia (three parts conc. hydrochloric acid to one part conc. nitric acid) and a known amount of copper carrier (about 100 mg.) was added, followed by hold-back carriers for cobalt, iron, manganese, chromium, vanadium, titanium, potassium and carbon. No scandium carrier was added owing partly to its cost and partly to the fact that titanium is an effective carrier for scandium. The hold-back carriers were present in about 100 mg. quantities each.

The copper carrier was in the form of a solution of cupric sulphate. The other carriers were cobalt chloride, ferric chloride, manganese carbonate chromium trioxide, ammonium metavanadate, titanium sulphate, potassium chloride, and ammonium carbonate. Wherever possible 'Analar' quality reagents were used. With the exception of ammonium carbonate, the solutions of these carriers in dilute acid were mixed and added to the target solution immediately after the addition of the copper carrier. Following this, solid ammonium carbonate was added and the mixture shaken vigorously. Carbon dioxide and ammonia were evolved.

The solution of target and carriers was filtered to remove traces of undissolved nickel. A pressure filter pump, large diameter buckner funnel and Whathams No. 5 filter papers were used to achieve rapid filtration. Owing to the necessary bulk of liquid present, centrifuging is not a practical alternative. Copper was precipitated from a molar solution of the filtrate as cupric and cuprous sulphide using hydrogen sulphide. None of the interfering elements are precipitated by hydrogen

sulphide in acid solutions. The precipitate was collected by filtering (using a different funnel to prevent contamination) and washed repeatedly with dilute hydrochloric acid and finally with water. The precipitate was folded up in the filter paper (No. 5) and placed in a copper box for counting. In general counting began on the separated copper less than 30 minutes after the end of the irradiation.

After the completion of counting, the filter paper was burnt in a silica crucible at normal bunsen heat and the final precipitate weighed to determine the efficiency of the chemical separation. When heated to a moderate temperature any sulphide present in the cupric form is converted into the more stable cuprous sulphide. That this happens at the temperature of the crucible was confirmed by separately heating known quantities of both sulphides in damp filter papers in the crucible. The weight of the final precipitate was generally about 150 mg. and the efficiency of separation around 95%

Dummy runs using no copper carrier and non-active targets showed that no other element was precipitated

in visually observable quantities by the chemical processing. A conclusive confirmation of the extraction of copper and no other element from the nickel target cannot be made other than by the use of active samples. Consequently several of the early synchrotron runs were devoted to perfecting the separation as described above.

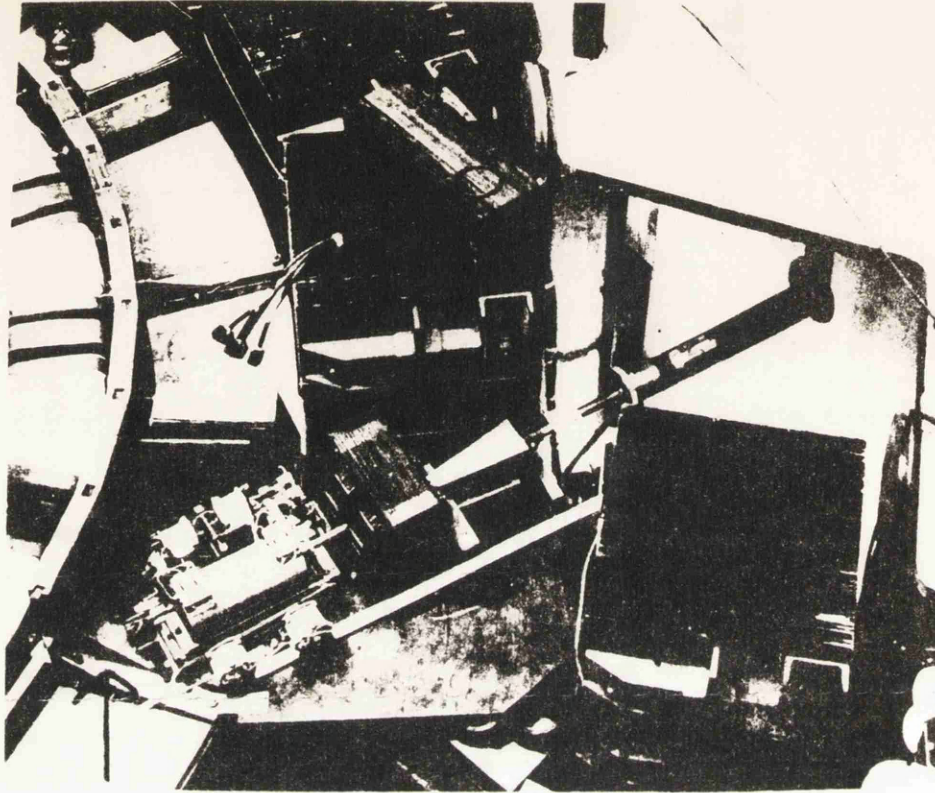
3.3 The Separation of Mn⁵² from a Chromium Target

The purest powder form of chromium available was 'Analog' chromium trioxide; the effects of the impurities are negligible. Since the half-life of the separated isotope Mn^{52m} is 21 minutes, the effect of C¹¹ produced by the reaction $O^{16}(\gamma, \alpha n)C^{11}$ will be appreciable. C¹¹ is a positron emitter with a half-life of 20.5 minutes. The spallation products Cr⁴⁹, V⁴⁷, Ti⁴⁵, Sc⁴⁴, Sc⁴³, K³⁸, and Cl³⁴ are likely interfering radio-isotopes (figure 3.1.) Titanium and scandium, having similar chemical properties to manganese may co-precipitate on the manganese. Fortunately Ti⁴⁵, Sc⁴⁴ and Sc⁴³ have fairly long half-lives (3 and 4 hours) and their presence in the final manganese decay curve will be readily observed. Steps can then

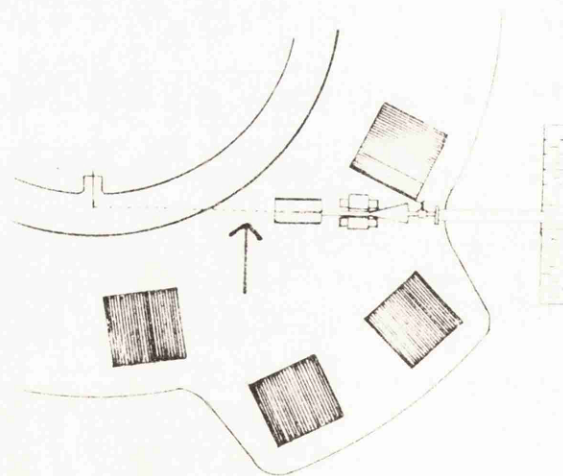
be taken to remove them.

The chromium trioxide target (of mass 20 g.) was dissolved in water and a known quantity of manganese carrier added in the form of a solution of manganese carbonate in dilute acid. Hold-back carriers for chromium, vanadium, titanium, potassium, chlorine and carbon were added as in the previous separation. The solution was filtered to remove traces of undissolved material using Whatmans No. 52 filter papers. Manganese and titanium (and some scandium by co-precipitation) were precipitated as manganous hydroxide and ortho-titanic acid by the addition of sodium hydroxide and sodium peroxide to the filtrate. Care was taken at this stage to keep the solution cool to prevent the formation of meta-titanic acid which is difficultly soluble in dilute mineral acids. The mixture was shaken to oxidise the manganous hydroxide to oxides of manganese. Again keeping the solution cool, hydrochloric acid was added until the mixture reached molar acid concentration. The oxidised manganese remained precipitated, whereas the ortho-titanic acid (and adsorbed scandium) dissolved.

The mixture was then filtered and the precipitate washed and folded up in the filter paper (No. 5) for counting. As in the previous separation dummy runs yielded no visible signs of other elements being precipitated. After counting the filter paper was burned and weighed as trimanganese tetroxide. The separation generally took about 35 minutes due to the necessity of keeping the solution cool. The efficiency of separation was poor (~35%) and this appeared to be due to loss of manganese when the titanium was redissolved. No titanium activity, however, was observed and so the separation was considered satisfactory. No steps were taken to improve the efficiency since it became clear that the upper isomeric state of Mn^{52} was not produced in measurable quantities.



FIGURES 4.1 and 4.2. The targets were irradiated between the internal synchrotron target and the collimator as shown.



4.1 Experimental Procedure

Natural boron powder (81.2% B^{11} and 18.8% B^{10}) of 99.5% purity in the form of an amorphous powder was packed uniformly into thin walled copper boxes of dimensions 1 in. x 1 in. x $\frac{1}{4}$ in. and exposed simultaneously with a 1 in. x 1 in. x $\frac{1}{8}$ in. piece of distrene (C_8H_8) placed immediately behind it. The exposure was made in the uncollimated bremsstrahlung beam of the Glasgow 330 MeV electron synchrotron for a period of one hour. The uncollimated beam was used since the intensity in it is less after collimation. The position of exposure is shown in figures 4.1 and 4.2.

The distrene acts as a monitor because the predominant reaction occurring in it is $C^{12}(\gamma, n)C^{11}$ resulting in the same residual nucleus as the reaction $B^{11}(\gamma, \pi^-)C^{11}$. Thus fluctuations in beam intensity during exposure are compensated for automatically by measuring the ratio of the activity produced in the boron sample to that produced in the distrene sample, since each receives the same intensity.

The decay scheme of C^{11} is quite simple: it decays with a half-life of 20.5 minutes to the ground state of B^{11} by the emission of a 0.96 MeV positron. After exposure the boron powder was transferred to another copper box of similar dimensions to the target and with walls thick enough to absorb the C^{11} positrons. This second box was placed between the two sodium iodide crystals of the initial detection system. The activities of the boron and distrene samples were initially displayed on a 100 channel kicksorter, from which it was seen that the spectrum of pulses were consistent with the C^{11} decay scheme. Using a scaler, the half-lives of the positron activities of the samples were measured by taking counts over several half-lives of C^{11} . The half-life of the positron activity produced in the boron was found to be 20.8 ± 0.6 minutes and that in the distrene 20.7 ± 0.7 minutes. These values are in good agreement with the value of 20.3 ± 0.1 minutes obtained by Barber, George and Reagan (1955) for the half-life of C^{11} . All these confirmatory tests were made with bremsstrahlung of maximum energy.

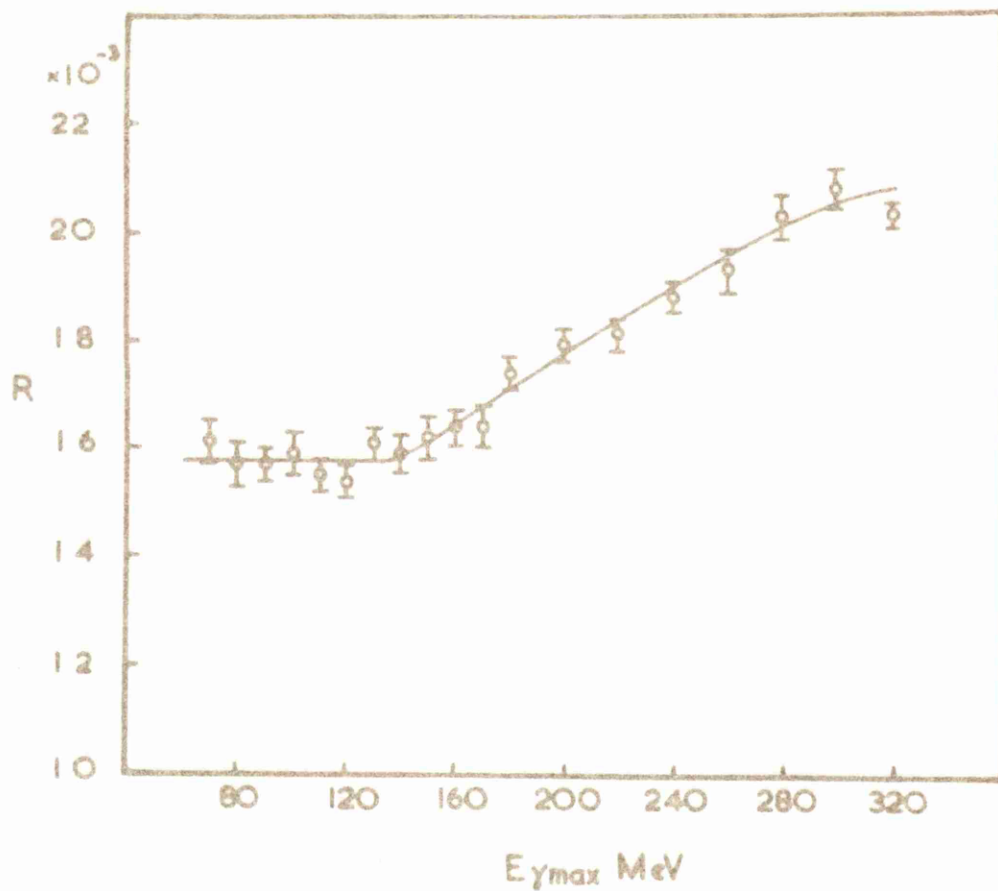


FIGURE 4.3. The ratio R of the β^+ activity per gram of boron to the β^+ activity per gram of distrene as a function of the peak energy of the Bremsstrahlung, $E_{\gamma\max}$.

Having verified that the observed activity was indeed that of C^{11} the ratio of the positron activity per gram of the boron sample to that of the distrene sample was measured at different maximum energies of the bremsstrahlung beam ranging from 70 MeV to 320 MeV. The ratio R of the positron activity per gram of the distrene sample is shown in figure 4.3 as a function of the maximum energy $E_{\gamma \text{ max.}}$ of the bremsstrahlung spectrum. If all the positron activity produced in the boron sample were due to the reaction $B^{11}(\gamma, \pi^-)C^{11}$ R should be zero when $E_{\gamma \text{ max.}}$ was below the threshold energy for meson production in boron (~ 140 MeV). However R has a constant value of 1.58×10^{-2} for values of $E_{\gamma \text{ max.}}$ between 140 MeV and 70 MeV the lowest energy at which significant counting statistics could be obtained. Above 140 MeV R increases to a value of 2.08×10^{-2} at 320 MeV.

The fact that R is constant at low energies and that the increase in R at high energies begins at meson production threshold suggests that the increase is due to meson production. Hence it seems reasonable to subtract the constant value of R found at low

energies from the values found above 140 MeV and to assume that the difference is due to the reaction $B^{11}(\gamma, \pi^-)C^{11}$. The cross-sections were determined by two different methods. In the first the results of Barber, George and Reagan (1955) for the cross-section of the reaction $C^{12}(\gamma, n)C^{11}$ are used and in the second the latter cross-section is determined experimentally by exposing a distrene sample in the collimated synchrotron beam and using a Cornell chamber to measure the incident flux. The bremsstrahlung spectrum used in obtaining these cross-sections was that for a tungsten target of 0.020 in effective thickness. The effective thickness was determined by a measurement of the angular distribution of the photon beam and is in agreement with measurements of the spectrum made with a pair spectrometer.

4.2 The Calculation of the Cross-Section.

It can be readily shown from the laws of radioactive decay that the number of active atoms N_0 with a decay constant λ at the end of an irradiation t_1 , is given by

$$N_0 = \frac{K}{\lambda} (1 - e^{-\lambda t_1})$$

where K is the production rate. The counting rate observed at a time t_2 after the end of the irradiation is given by

$$\left(\frac{dN}{dt}\right)_{t_2} = K f (1 - e^{-\lambda t_1}) e^{-\lambda t_2} \quad \text{--- (A)}$$

where f is the fraction of the total disintegrations detected by the counting system.

Now,

K = no. of atoms/cm² × cross-section × total no. of effective quanta/unit time

$$= \int_{E_{\min.}}^{E_{\max}} N \frac{\sigma_E Q_E}{t} dE \quad \text{where}$$

Q_E is the number of quanta of energy E and t is the duration of the irradiation.

If the threshold energy for the monitoring reaction is essentially zero, the rate of production of active atoms in the monitoring sample is

$$K_M = \int_0^{E_{\max}} N_M \frac{\sigma_E Q_E}{t_1} dE$$

For pion production from a target of N_{π} atoms/cm² is

$$K_{\pi} = \int_{140\text{MeV}}^{E_{\max}} N_{\pi} \frac{\sigma_E Q_E}{t_1} dE$$

If the final nuclei of the meson and monitoring reactions are identical then the ratio of the production rates is

$$R = \frac{K_{\pi}}{K_M} = \frac{\left(\frac{dN}{dt}\right)_{\pi}}{\left(\frac{dN}{dt}\right)_M} = \frac{N_{\pi} \int_{140}^{E_{\max}} Q_E \sigma_E dE}{N_M \int_0^{E_{\max}} Q'_E \sigma'_E dE}$$

The cross-section for the meson reaction, then, averaged over the energy interval 140 MeV to E_{\max} is

$$\sigma(140 \rightarrow E_{\max}) = \frac{R K_M t_1}{N_{\pi} \int_{140}^{E_{\max}} Q_E dE}$$

$\int Q_E dE$ can be determined from the spectrum shape of the bremsstrahlung beam and K_M from relation A for a steady production rate. Alternatively, $\int N_M \sigma'_E dE$ can be calculated using known values of σ'_E . For these two evaluations of K_M , the respective cross-sections are given by

$$\sigma(140 \rightarrow E_{\max}) = \frac{R t_1 K_M f e^{-\lambda t_2} (1 - e^{-\lambda t_1})}{N_{\pi} \int_{140}^{E_{\max}} Q_E dE} \quad \text{--- (B)}$$

or

$$\sigma(140 \rightarrow E_{\max}) = R \cdot \frac{NM \int_0^{E_{\max}} Q_E \sigma_E dE}{N\pi \int_{140}^{E_{\max}} Q_E dE} \dots \textcircled{C}$$

$\sigma(E_2 \rightarrow E_1)$ can readily be determined from $\sigma(140 \rightarrow E_2)$ and $\sigma(140 \rightarrow E_1)$ by the photon difference method.

There are, therefore, two methods of evaluating the required cross-section. In the first the ratio of the counting rates are determined for the target and monitoring activities. A further calibration run is performed in which the monitoring sample is exposed to a steady beam for a known number of equivalent quanta. The efficiency factor, f , which includes both counter efficiencies and solid angle factors is determined by standard methods. The experimental run and the calibration run are normalised using the definition of equivalent quanta n ,

$$\text{i.e. } n = \frac{\int_0^{E_{\max}} Q_E \cdot E dE}{E_{\max}}$$

The cross-section is then determined by equation B.

In the second method it is sufficient to measure

TABLE 4.1

Photon Energy (μeV)	140-170	170-200	200-230	240-260	260-290	290-320
Calculated σ_v	17.3	21.5	19.0	15.2	12.0	9.6
Calculated τ_s	2.7	3.8	3.2	2.5	2.1	1.8
Measured σ	2.7	2.7	2.7	3.1	2.9	2.2

the activity ratio and to use a bremsstrahlung spectrum shape and published values of the cross-section of the monitoring reaction. The accuracy of this method relies principally on the spectrum shape assumed and on the accuracy of the reported carbon cross-section. The first method is less sensitive to spectrum error but can only be used at energies for which the Cornell chamber (for determining the number of equivalent quanta) is calibrated.

4.3 Results

The values obtained for the cross-section of the reaction $B^{11}(\gamma, \pi^-)C^{11}$ averaged over the photon energy range 140 to 320 MeV are $(2.6 \pm 0.2) \times 10^{-29} \text{ cm}^2$ and $(2.9 \pm 0.2) \times 10^{-29} \text{ cm}^2$ using respectively, the published and experimental values of the cross-section of the reaction $C^{12}(\gamma, n)C^{11}$. The cross-section was also determined as a function of photon energy using the mean values of the average cross-sections given by the two methods. The values were averaged over 30 MeV intervals from 140 to 320 MeV. In table 4.1, the cross-section is compared with the theoretical

values for surface production.

Since the agreement is good between the values obtained by both methods of calculation, in the following nickel measurements only the first method was used. In this the cross-section of the monitoring reaction and the shape of the bremsstrahlung spectrum are assumed.

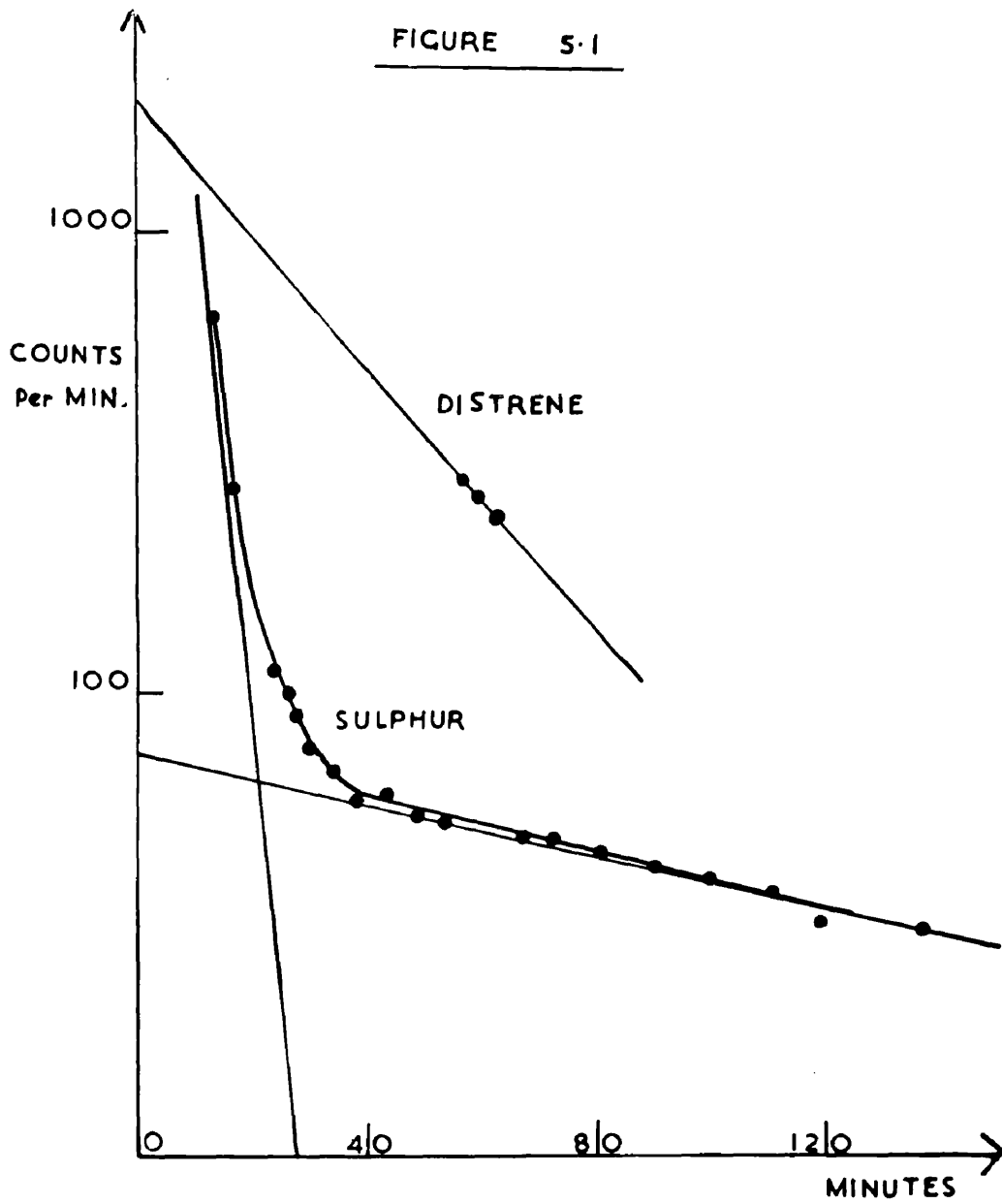


FIG. 5.1 A TYPICAL SULPHUR DECAY CURVE

CHAPTER FIVE(γ , π^-) REACTIONS IN SULPHURCHROMIUM AND NICKEL5.1 The Reaction $S^{34}(\gamma, \pi^-)Cl^{34}$.

Of the product nuclei of reactions of the type $X(\gamma, \pi^-)Y$ on natural sulphur (S^{32} - 95%; S^{33} - 0.75%; and S^{34} - 4.2%) only Cl^{34} has a half-life greater than a few seconds. Cl^{34} decays by positron emission with a half-life of 33 minutes. The experimental procedure adopted for the detection of the Cl^{34} activity from the reaction $S^{34}(\gamma, \pi^-)Cl^{34}$ is essentially the same as that of the previous chapter.

Natural sulphur of 99.9% purity was melted in a clean dry pyrex crucible and poured into 1 in x 1 in x $\frac{1}{4}$ in moulds. The resulting blocks were irradiated along with distrene samples in the uncollimated bremsstrahlung beam. The positron activities of the sulphur and distrene samples were observed as in the boron work. A typical decay curve of the sulphur activity is shown in figure 5.1. The activity is consistent with two half-lives of 2.5 minutes and 112 minutes corresponding to the positron emitting isotopes P^{30} and F^{18} . There was no indication of a 33 minute half-life.

If the cross-sections of the reactions of the type $X(\gamma, \pi^-)Y$ obey the $A^{2/3}$ law of meson production, then the activity to be expected from the reaction $S^{34}(\gamma, \pi^-)Cl^{34}$ can be deduced from the $B^{11}(\gamma, \pi^-)C^{11}$ measurements. At a peak bremsstrahlung energy of 240 MeV, the observed activity of F^{18} is twenty times the expected Cl^{34} yield rendering the detection of Cl^{34} by this method impossible. Owing to the low isotopic abundance (4.2%) of S^{34} in natural sulphur, the high yields of P^{30} and F^{18} and the difficulties involved in a chemical separation of chlorine and fluorine, no further attempts were made to observe the reaction $S^{34}(\gamma, \pi^-)Cl^{34}$.

The measurements made on the F^{18} activity from natural sulphur are included in the photospallation studies of chapters 9 and 10. It was the unsuspected high yield of F^{18} which prompted these studies.

5.2 The Reaction $Cr^{52}(\gamma, \pi^-)Mn^{52m}$

Manganese-52 has an isomeric state of half-life 21 minutes which decays by positron emission (99+%) to stable Cr^{52} and by an internal transition (0.05%)

to the 5.6 day ground state of Mn^{52} . A measurement of the activity of the 21 minute isomer will determine to what extent it is produced in a (γ, π^-) reaction on Cr^{52} .

Chromium trioxide was packed into one inch perspex cubes and irradiated between polythene (C H_2) monitoring discs in the uncollimated bremsstrahlung beam of the synchrotron. The target was treated as in chapter 3 to separate the active manganese. The activity of the resulting manganese was examined using the modified positron detection system.

No activity corresponding to a half-life of 21 minutes was observed. There was, however, the persistent appearance of a positron activity of half-life about 40 minutes. This may be due to V^{47} (half-life; 33 min.) and Cr^{49} (half-life; 42 min.) arising from inefficient chemical separation. Alternatively it may be due to Mn^{51} (half-life; 44 min.) produced by the reaction $\text{Cr}^{52}(\gamma, \pi^-n)\text{Mn}^{51}$. The criterion for a satisfactory radiochemical separation is that the only activity observed is that of the required element. Owing to the similarities

in the decay properties of Cr^{49} and Mn^{51} , at no time could absolute certainty be reached that the observed activity was due solely to Mn^{51} . It is thought unlikely that the activity is due principally to Cr^{49} and V^{47} because of the successful dummy runs and of the great mass ratio of the original chromium target to the final precipitate. It is also not known to what extent the 40 minute activity masks the investigated 21 minute activity.

Although these investigations were preliminary it appeared that the cross-section varied appreciably with incident photon energy. A (γ, n) or similar reaction would not be expected to show much variation. These measurements suggest that the cross-section of reaction $\text{Cr}^{52}(\gamma, \pi^-)\text{Mn}^{52m}$ is not significant and also that (γ, π^-n) reactions may have observable cross-sections.

5.3 The Reaction $\text{Ni}^{60}(\gamma, \pi^-)\text{Cu}^{60}$

In natural nickel, Ni^{60} is 26% abundant and the product nucleus from a (γ, π^-) reaction on it is a positron emitter of 24 minutes half-life. Nickel would then appear suitable for a study of the (γ, π^-)

reaction.

In preliminary runs, several high purity nickel discs of area one square inch were irradiated with a distrene sample and the resulting positron activities examined. The observed decay curve showed that a quantitative assignment of an activity of half-life 24 minutes was impossible and that a mixture of many activities was present. Further the counting rate was about 200 times greater than that expected for the yield from the reaction $\text{Ni}^{60}(\gamma, \pi^-)\text{Cu}^{60}$ on the basis of an extrapolation from the yield of C^{11} from the reaction $\text{B}^{11}(\gamma, \pi^-)\text{C}^{11}$. This demonstrated the necessity for chemical separation of the Cu^{60} activity, the description of which appears in chapter 3.

Each nickel sample consisted of 12 grams of fine nickel powder packed into a perspex box of dimensions 1 in. x 1 in. x $\frac{1}{4}$ in. The sample was irradiated between two pieces of polythene (CH_2), each 1 in. x 1 in. x $\frac{1}{16}$ in., in the uncollimated synchrotron beam. The reaction $\text{C}^{12}(\gamma, n)\text{C}^{11}$ occurring in the polythene was again used to monitor the beam

intensity and also to measure the absorption in the nickel sample. During the irradiation a continuous record was made of the beam intensity. This is necessary since Cu^{60} has a different half-life from the monitoring C^{11} activity. The samples were irradiated for an hour in a flux of approximately 10^{10} equivalent quanta per minute.

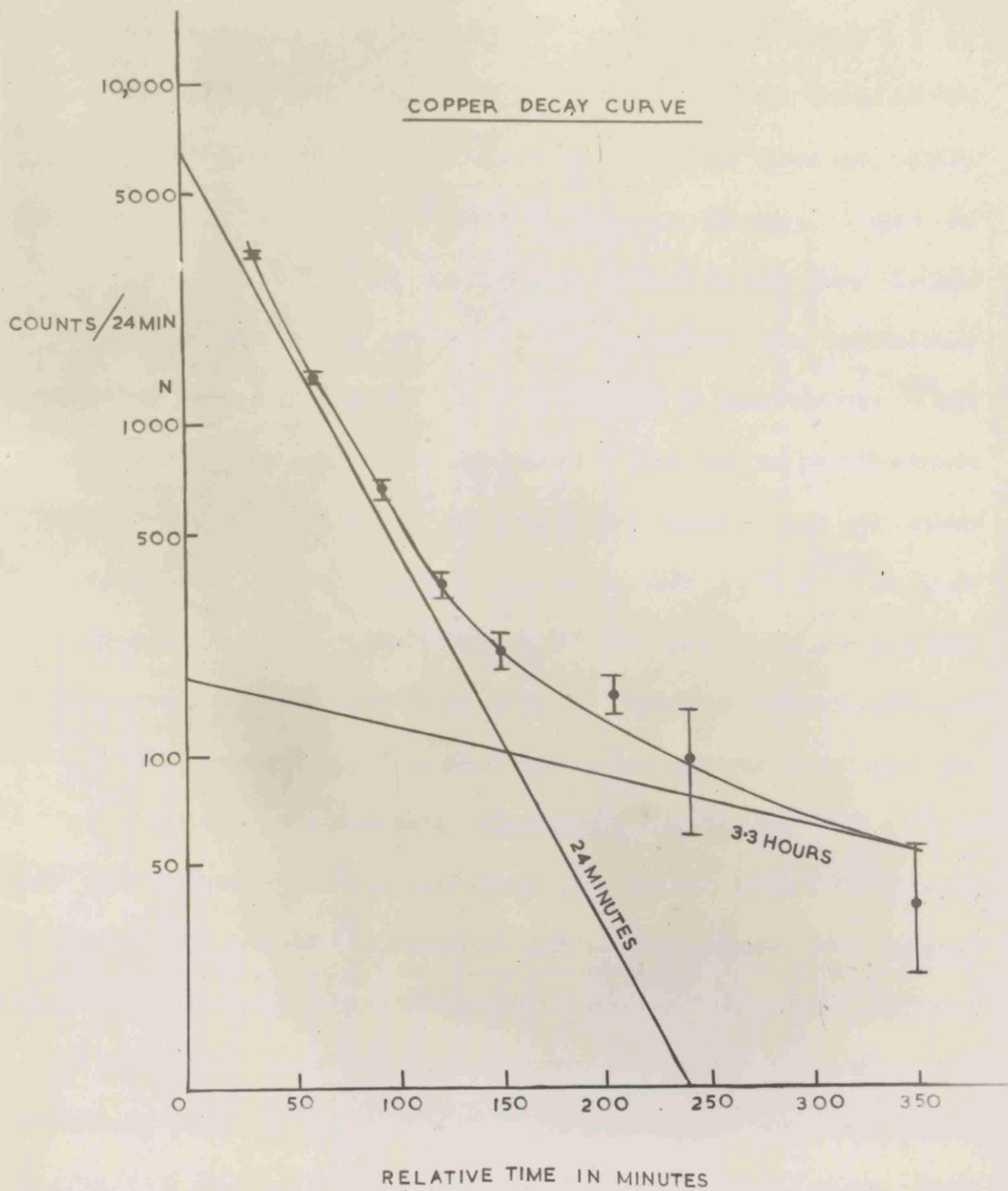
After exposure the nickel sample was removed from the perspex box and dissolved in aqua regia. A chemical separation of the copper activity was made and the resulting copper sulphide precipitate was folded up in the filter paper. This was placed in a copper box of dimensions 1 in. x 1 in. x $\frac{1}{4}$ in. with walls thick enough to absorb the highest energy positrons (3 MeV) from the Cu^{60} decay. The positron activity of Cu^{60} was measured using the modified detection system. In general, counting began on the separated copper about 28 minutes after the end of the irradiation and continued for an hour. After counting, the efficiency of the separation was determined by weighing the copper precipitate after ignition at a moderate heat.

In view of the very low cross-section for the

(γ, π^-) ~~cross-section~~ ^{process} compared to spallation processes it is necessary to confirm that the activity observed is in fact due to Cu^{60} . The most abundant isotope of nickel is Ni^{58} (67.9%) but a (γ, π^-) reaction in this isotope results predominantly in the formation of the 3 second isomer of Cu^{58} . The (γ, π^-) reaction which was observed occurred in Ni^{60} (26.2%) the positron emission detected being from the decay of Cu^{60} which has a half-life of 24 minutes. A small contribution to the activity observed will have been made by the other isotopes Ni^{62} (3.7%), Ni^{61} (1.2%) and Ni^{64} (1%), the product nuclei Cu^{62} , Cu^{61} and Cu^{64} having half-lives of 10.1 minutes, 3.3 hours and 12.8 hours, respectively. The principal decay properties of the copper isotopes is shown in figure 5.2.

A (γ, π^-) reaction proceeds diagonally upwards to the left, the lower nuclide being the target and the upper the product. The contribution of the other nickel isotopes to the observed activity was estimated by assuming that the cross-section was the same as that for the reaction $\text{Ni}^{60}(\gamma, \pi^-)\text{Cu}^{60}$; the contribution was estimated to be about 10% in a typical irradiation

FIGURE 53



and is mainly due to the 10.1 minute and 3.3 hour activities.

The first check is that of the half-life of the observed activity. The decay curve of the copper activity produced by bremsstrahlung having a maximum energy of 320 MeV is shown in figure 5.3. The contribution of the 10.1 minute activity produced by the reaction $\text{Ni}^{62}(\gamma, \pi^-)\text{Cu}^{62}$ from Ni^{62} (3.7%) was found to be about 7.5% of the counting rate at 34 minutes, 2% at 62 minutes and negligible for subsequent observations. The remaining activity is consistent with a 95% component of half-life 24 minutes and a 5% component of half-life 3.3 hours. The 3.3 hour activity was greater than expected and was presumably due to the reaction $\text{Ni}^{61}(\gamma, \pi^-)\text{Cu}^{61}$ on Ni^{61} (1.2%) and possibly also to $\text{Ni}^{62}(\gamma, \pi^-n)\text{Cu}^{61}$.

A conclusive identification of the Cu^{60} activity can be made by measuring the γ -ray spectrum following the positron emission. Its two major components both involve positron emission followed by two γ -rays in coincidence, the energy of both γ -rays being greater than that of the annihilation quanta (0.51 MeV). In

none of the spallation products of similar half-life does this occur. Thus a comparison of the number of pulses in the photo-electric peak due to annihilation quanta, with the number of pulses having a greater pulse height will yield different results for positron emission, (a) without subsequent γ -ray emission, (b) with a single coincident high energy γ -ray and (c) with two coincident high energy γ -rays. The

TABLE 5.1

Isotope	Number of Pulses		Ratio of Number of Pulses $\frac{> \text{Peak}}{\text{Peak}}$
	P.E. Peak	Peak	
^{11}C	2178 ± 47	17 ± 9	0.0078 ± 0.0042
^{22}Na	2277 ± 48	481 ± 23	0.211 ± 0.012
^{60}Cu	1276 ± 40	506 ± 30	0.396 ± 0.026

having a maximum energy of 320 MeV. ^{11}C is a pure positron emitter and the ^{22}Na emission is followed by a single γ -ray of energy 1.28 MeV. A direct comparison can be made between the ^{22}Na and ^{60}Cu results because the efficiencies of detection of the high energy γ -rays are similar and therefore, assuming that the γ -rays are emitted in random directions, the

none of the spallation products of similar half-life does this occur. Thus a comparison of the number of pulses in the photo-electric peak due to annihilation quanta, with the number of pulses having a greater pulse height will yield different results for positron emission, (a) without subsequent γ -ray emission, (b) with a single coincident high energy γ -ray and (c) with two coincident high energy γ -rays. The latter possibility can only occur in the present experiment if the activity is due to Cu^{60} . The experimental values obtained for the number of pulses in the photo-electric peak of the annihilation quanta and the number of pulses of greater pulse height for C^{11} , Na^{22} and the separated copper activity are given in table 5.1 for irradiations with bremsstrahlung having a maximum energy of 320 MeV. C^{11} is a pure positron emitter and the Na^{22} emission is followed by a single γ -ray of energy 1.28 MeV. A direct comparison can be made between the Na^{22} and Cu^{60} results because the efficiencies of detection of the high energy γ -rays are similar and therefore, assuming that the γ -rays are emitted in random directions, the

ratio found for Cu^{60} should be approximately twice that for Na^{22} . The results show conclusively that the positron activity of the separated copper is followed by two high energy γ -rays in coincidence thus confirming the activity as due to Cu^{60} . These results on the spectra of pulses observed for the different activities also gave a direct measurement of the relative efficiencies for the detection of the C^{11} and Cu^{60} activities.

The only major modification of the value observed for the ratio of the Cu^{60} activity to the C^{11} activity is due to the different efficiencies for counting the two activities. This difference arises because the positron decay of C^{11} goes directly to the ground state of B^{11} whereas the positron decay of Cu^{60} goes to excited states of Ni^{60} which subsequently decay by γ -ray emission to the ground state. These γ -rays are in coincidence with the quanta resulting from the annihilation of the positrons and increase the efficiency for detecting the Cu^{60} activity. This increase of efficiency was determined experimentally to be 40%.

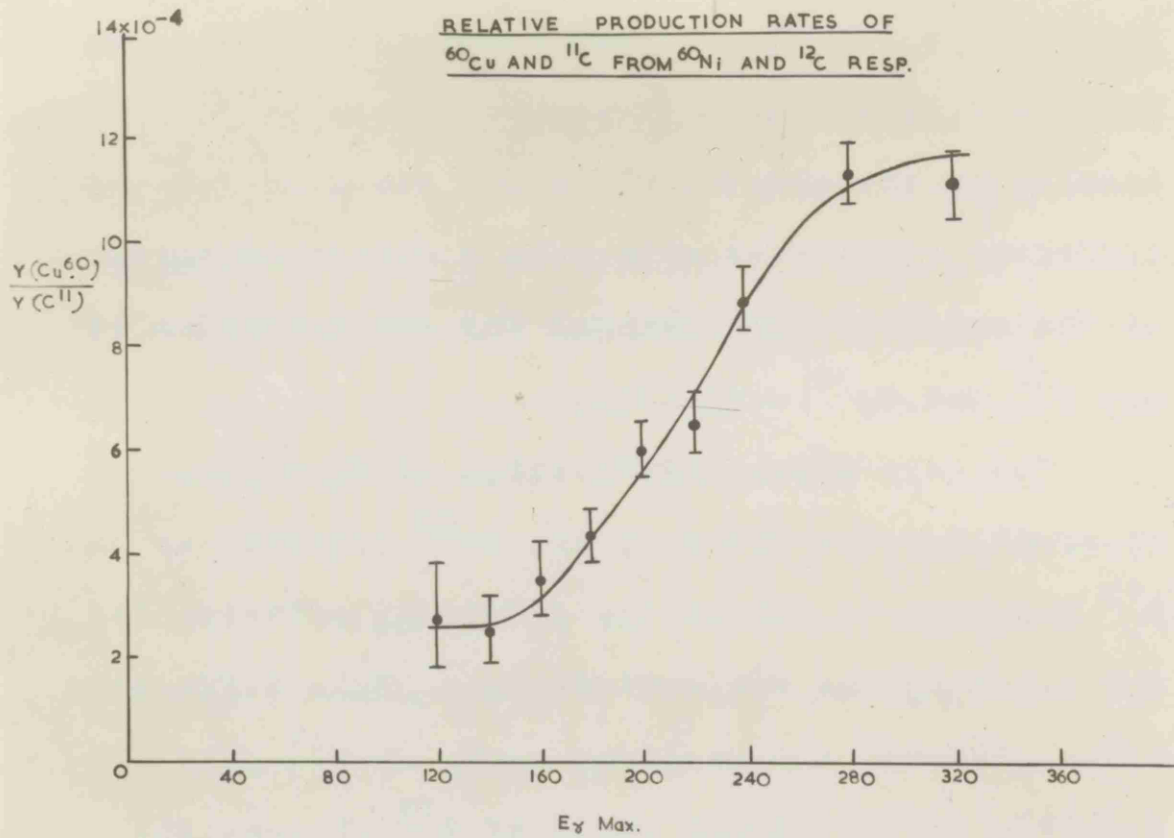


FIGURE 5-4

For each irradiation the positron activity of the separated copper and of the polythene monitor were measured. After making allowance for the efficiency of the chemical separation and beam fluctuations, the ratio was determined of the positron activity of Cu^{60} produced per gram of nickel sample to the positron activity of C^{11} per gram of C^{12} in the polythene. The measurements were made with bremsstrahlung having maximum energies ranging from 120 to 320 MeV.

The ratio of the production rate of Cu^{60} per atom of Ni^{60} to that of C^{11} per atom of C^{12} is shown in figure 5.4 as a function of the maximum energy of the bremsstrahlung. It is very small at energies below the threshold for meson production and rises at higher energies to a value four times greater at 320 MeV. The counting rates obtained with bremsstrahlung of maximum energy 140 MeV and 120 MeV were too low to obtain significant determinations of the half-life or pulse height spectrum of the activity. The values given at these energies were based on the assumption that all the observed activity

TABLE 5.2

Photon Energy (MeV)	140-170	170-200	200-230	230-260	260-290	290-320
Cross-section for ^{60}Ni (γ, π^-) $\text{Cu}^{60}(\text{cm}^2)$	2.2 ± 0.4	4.2 ± 0.5	6.1 ± 0.5	5.9 ± 0.6	2.6 ± 0.7	0.2 ± 1.2

was due to Cu^{60} .

The cross-section for the reaction $\text{Ni}^{60}(\gamma, \pi^-)\text{Cu}^{60}$ was obtained from the ratio of the production rates by using the results of Barber, George and Reagan (1955) for the cross-section of the reaction $\text{C}^{12}(\gamma, n)\text{C}^{11}$ and assuming a bremsstrahlung spectrum for a tungsten target of 0.020 in effective thickness as outlined in chapter 4. Table 5.2 shows the cross-section as a function of photon energy averaged over 30 MeV intervals.

CHAPTER SIX THE ACTIVITY BELOW THRESHOLD

The threshold energy for the photoproduction of a free meson from a complex nucleus is about the rest energy of the meson (~ 140 MeV). Consequently, any activity produced by photons of energy less than 140 MeV cannot be the result of free meson production. In the boron measurements the activity observed below threshold was 75% of the total activity observed at 320 MeV and for nickel it was at the most 25% the 320 MeV activity. Investigations of possible sources of these activities were made.

The activity observed in boron below threshold was observed to have the half-life and γ -ray spectrum of C^{11} . In figure 4.3 the ratio R of the positron activity per gram of the boron sample to the positron activity per gram of the distrene sample was given as a function of the maximum energy $E_{\gamma \text{ max.}}$ of the bremsstrahlung spectrum. The reactions expected to produce these activities are $B^{11}(\gamma, \pi^-)C^{11}$ and $C^{12}(\gamma, n)C^{11}$ respectively and R should be zero when E_{γ} was less than 140 MeV. R , however, has a constant value of 1.58×10^{-2} for values of $E_{\gamma \text{ max.}}$ between

140 MeV and 70 MeV. Clearly an impurity of 1.58% carbon in the boron sample would be sufficient to account for all the observed activity below threshold. However, the carbon content of the boron was quoted by the manufacturers to be less than 0.1%. During and after the experimental runs further analyses were made using a mass spectrometer. In each case the maximum carbon impurity was given as 0.3%. The manufacturer's analysis listed impurities of about 0.1% each of magnesium, aluminium, manganese, iron and oxygen. All these elements were irradiated and the resulting positron activities compared with that produced in the boron below threshold. The results showed that at least 30% of any of these elements would be necessary to produce the activity found in the boron at low energies. It, thus, seems improbable that impurities are the cause of this activity.

Another possibility is the production of C^{11} by the interaction with boron of secondary particles generated by the bremsstrahlung. The most probable reactions being $B^{11}(p,n)C^{11}$ and $B^{10}(p,\gamma)C^{11}$. It was found that R was uncharged when the boron sample was

shielded by various thicknesses of lead and copper and when the material used for the container was changed. R was also unchanged when the irradiation was made behind a 10,000 gauss scrubbing magnet. Thus protons originating outside the sample are not responsible.

For photoprotons produced in the boron sample itself and having a range greater than the thickness of the sample, the number of C^{11} nuclei produced by two stage processes such as $B^{11}(\gamma, p)Be^{10}$ followed by $B^{11}(p, n)C^{11}$ should vary approximately as the square of the sample thickness. For a single stage reaction such as $B^{11}(\gamma, \pi^-)C^{11}$ the variation should be linear. It was found experimentally that the variation with sample thickness was linear for all thicknesses used (1 cm to 0.1 cm). If the range of the photoprotons were less than 0.1 cm in the boron sample, then their energy would be less than 8 MeV and the cross-sections for the (γ, p) and (pn) reactions in boron would be much too small to produce the activity observed. Thus the obvious sources of the positron activity at low energies cannot account for the magnitude of the

effect observed.

The ratio of the production rates of Cu^{60} per atom of Ni^{60} to that of C^{11} per atom of C^{12} was shown in figure 5.4 as a function of the maximum energy of the bremsstrahlung. It is very small at energies below meson threshold and rises at higher energies to a value four times greater at 320 MeV. The value at threshold is about eight times smaller than that observed in the boron measurements. The counting rates obtained with bremsstrahlung of maximum energy 140 MeV and 120 MeV were too low to obtain significant determinations of the half-life or pulse height spectrum of the activity produced at these energies. As far as the values of figure 5.2 are concerned, the activity observed below meson threshold has been assumed to that of Cu^{60} . The activity must have a half-life very similar to that of Cu^{60} , otherwise its presence might have been observed in the decay curve obtained at 320 MeV.

The nickel impurities are oxygen 0.1%, carbon 0.05 - 0.1%, iron 0.01% and sulphur 0.001%. Of these only carbon is present in quantity sufficient to produce detectable activity below meson threshold.

The activity observed may, than, be due to the 20.5 minute positron activity of C^{11} produced by the reaction $C^{12}(\gamma, n)C^{11}$. The chemical separation procedure should, of course, eliminate any carbon from the final copper precipitate. It was expected that most of the active carbon would have been lost when carbon dioxide was given off. It is possible that the carbonate or carbon dioxide did not remain in the solution long enough to mix with all the active carbon. The remaining carbon may, then, become adsorbed on the final precipitate or filter paper. If this were so carbon would also be adsorbed at the first filter stage. It appears difficult to explain the observed activity totally on the ground of carbon impurity.

Another source of activity could be the co-precipitation or adsorption of positron emitting nuclides produced by spallation reactions on nickel on to either the copper precipitate or the final filter paper. Owing to the large quantity of active material in solution this may be a source of some of the observed activity. To eliminate the possibility of such activities the final precipitate was washed

with large volumes of weak acid and finally with water. It was not possible to determine whether this washing was successful or not. An inspection of the periodic table shows that if spallation products are the source of the activity, then it would be expected that the apparent half-life would be long, due to the predominance of long-lived isotopes of nickel and cobalt in the solution. It is possible that the adsorption is selective in favour of other nuclides such as iron, manganese etc., the combined effect of which would be to show no strong half-life other than that of 20-30 minutes. It seems possible, then, to attribute some of the observed activity to the chemical processing.

Since the observed activity was very small at low energies it was not possible to measure the effects of target thickness on the counting rates. The possibility of two-stage processes cannot therefore be eliminated. Although the total activity is small and may be explained in terms of several effects, it is possible that it may be produced in a similar manner to the activity observed from boron below threshold.

In the evaluation of the (γ, π^-) cross-sections in boron and nickel it was assumed that the ratios of the low energy activity to the monitoring activity remained constant above threshold. If the activities are produced by (γ, n) reactions in impurities or (γ, p) two-stage reactions in the samples then the ratios would be expected to remain constant for energies well above the resonances (~ 20 MeV). It will be shown in the photospallation studies (chapter 10) that the ratios of spallation reactions to (γ, n) processes is approximately constant for energies greater than about 140 MeV. The assumption, then, that the low energy activity remains constant relative to the (γ, n) monitoring activity seems quite justifiable.

If the observed activities are due to C^{11} and Cu^{60} , reactions of the type (γ, e^-) on B^{11} and Ni^{60} could produce them. Such reactions have not been reported and would not be expected to have a large cross-section. The cross-section required to explain the boron activity by such a reaction would be of the order of 10^{-28} cm².

In conclusion, it appears that the activity observed below meson threshold from nickel may be explained by the chemical processing. The activity is, however, small. The sources of the activity from boron, on the other hand, remain unexplained. As far as the interpretation of the (γ, π^-) yields are concerned, the activities below threshold have been treated as background effects.

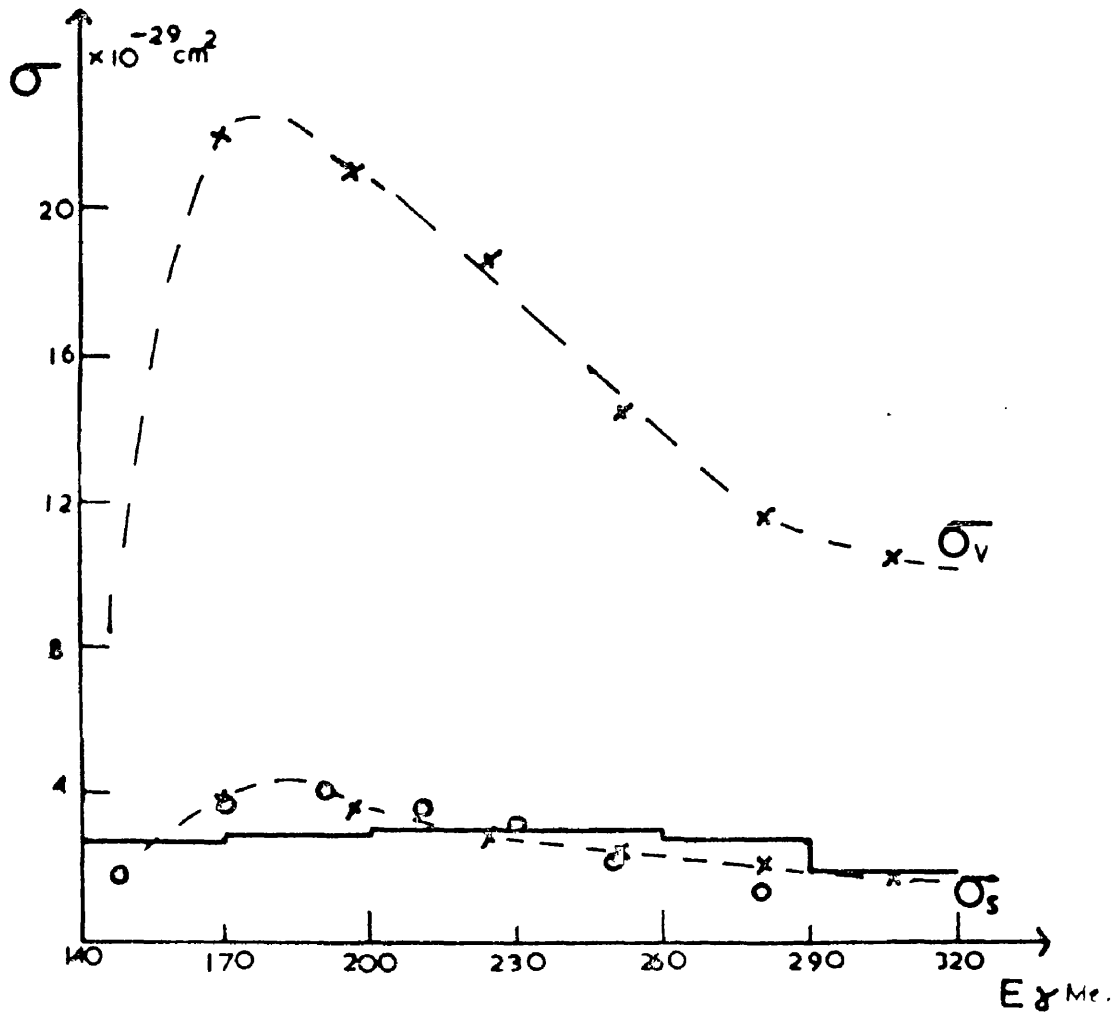


FIGURE 7A. The cross-section of the reaction $B^{11}(\gamma, n^-)C^{11}$ as a function of incident photon energy averaged over 10 keV intervals. See text for legend.

CHAPTER SEVENDISCUSSION7.1 The Cross-sections as a Function of Energy

Laing and Moorhouse (1957) have calculated values of the cross-section for the reaction $B^{11}(\gamma, \pi^-)C^{11}$ for production from the surface nucleons only and also throughout the nuclear volume. In figure 7.1, dotted curves $\overline{\sigma}_S$ and $\overline{\sigma}_V$ are drawn through their calculated values for surface and volume production, respectively. The experimental values have been averaged over 30 MeV intervals and these are shown as solid lines. The errors of the present values are $\pm 20\%$. Recently, preliminary experimental values have been reported by Hummel and Dyal (1959) using a similar technique. Their results are indicated on figure 7.1 by circles. It can be seen that the experimental values are in very good agreement with the calculated values based on the surface production model. The calculated cross-section shows a maximum around 180 MeV incident photon energy. This result, however, may be model dependent since only S-wave production has been considered. The position of the experimental cross-section maximum cannot be determined since the

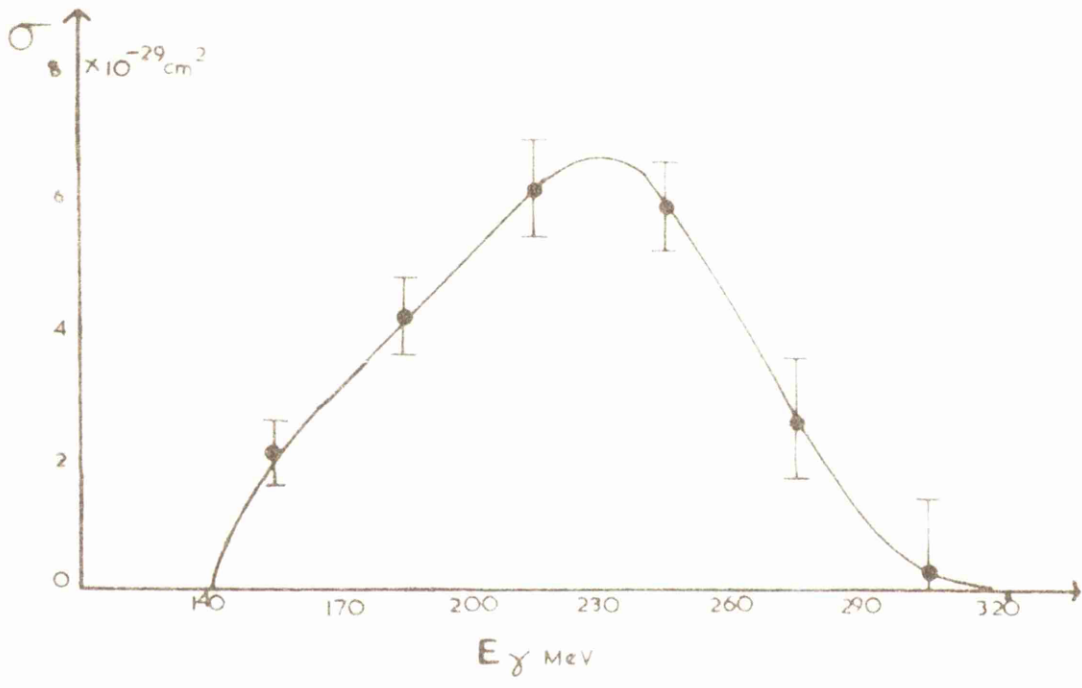


FIGURE 72. The cross-section of the reaction $\text{Ni}^{60}(\gamma, \pi^-)\text{Cu}^{60}$ as a function of incident photon energy averaged over 30 MeV intervals.

errors are greater than the differences in the cross-sections. It is apparent, however, that the cross-section decreases appreciably above 260 MeV. This is in contrast to the cross-section for the photoproduction of pions from free nucleons which has a maximum in the region of 300 MeV - the well known $(3/2, 3/2)$ resonance for P-wave mesons.

The variation of the $\text{Ni}^{60}(\gamma, \pi^-)\text{Cu}^{60}$ cross-section with photon energy is shown in figure 7.2. Again the cross-section has been averaged over 30 MeV intervals from 140 to 320 MeV. The curve rises to a maximum at 230 MeV and shows signs of symmetry about this energy. The lowest value of the cross-section appears at the highest energy interval as in the boron curve. Errors are shown at the middle energy of the interval, the largest errors appearing at the highest energies where the photon difference method is least accurate.

It has been assumed throughout that photopions are produced at a single nucleon in the nucleus. It might then be expected that photoproduction from a nucleon in a nucleus might also show the $(3/2, 3/2)$

resonance of production at a free nucleon. From the data presented by Williams, Crowe and Friedman (1957) it can be seen that for 550 MeV bremsstrahlung the maximum pion yield occurs for π^+ mesons of energy 115 MeV from hydrogen and 80 MeV from carbon and copper at a laboratory angle of 60° . From a consideration of the kinematics of the elementary process and neglecting the effect of the other nucleons, it would appear that these maxima correspond to photon energies of about 290 and 250 MeV for production from free and bound protons, respectively. The present results indicate a maximum around 230 MeV.

Due to the spread in momenta of nucleons in a complex nucleus, there exists no unique photon energy corresponding to a given energy and angle of emission of the pion. Instead there corresponds a band of photons available for pion production. It is for this reason that photoproduction from a complex nucleus is possible at photon energies down to about 10 MeV below the threshold for production from free nucleons. Secondly, for a given energy and angle of emission of the pion, the average energy of the photons

available for production from a complex nucleus is different from that from a free nucleon. This difference depends on the binding energies of the nucleons in the nucleus, and the interactions of the recoiling nucleons and pions with the product nucleus, including the Coulomb interaction. The observed shift of the cross-section maximum may then be a result of the properties of the complex nucleus.

The maximum may appear at an even lower energy for the case in which the recoiling nucleon remains bound in the nucleus, i.e. for reactions such as $B^{11}(\gamma, \pi^-)C^{11}$ and $Ni^{60}(\gamma, \pi^-)Cu^{60}$. The lower the energy of the recoiling nucleon the greater is the probability of it remaining in the nucleus. It may not have sufficient energy initially to penetrate the Coulomb barrier, or it may lose energy by collisions with other nucleons to form a compound nucleus. If this nucleus is de-excited by γ -ray emission then a (γ, π^-) reaction will be observed. If however the recoiling nucleon is emitted or causes other nucleons to be emitted either by direct collision or by the

decay of a compound nucleus, then a (γ, π^-) reaction will not be observed. Obviously since a low energy photon cannot produce a high energy recoil, there will be a greater probability of producing a (γ, π^-) reaction for lower photon energies. This will further move the position of ^{the} χ cross-section ^{maximum} for a (γ, π^-) reaction compared with that from free nucleons to lower energies.

It appears, then, the position of the observed maximum is quite consistent with the known properties of photoproduction. The agreement between the experimental values and the calculated "surface production" cross-section is good. A comparison of the shapes of the calculated cross-section and the B^{11} and Ni^{60} curves suggest that P-wave mesons also contribute to the cross-section of the reaction (γ, π^-) particularly for heavier nuclei.

7.2 The cross-sections as a function of mass number

It has been shown in chapter 1 that there are two competing theories for photoproduction from complex nuclei. Each is based upon the assumption that production occurs at a single nucleon. If

pions were produced at each nucleon of the nucleus one would expect the cross-section to be proportional to the number of nucleons i.e. A . However it has been observed that the cross-section is proportional to $A^{2/3}$. Butler (1952) proposed that production occurred only at surface nucleons and was suppressed in the core by a competing photodisintegration process (Wilson 1952). Thereby he has been able to explain the $A^{2/3}$ trend and also the π^-/π^+ ratios. This model was further supported by George (1952) with evidence from the photoproduction of pions in nuclear emulsions. On the other hand Francis and Watson (1953) showed that by considering the mean free path for the absorption of pions in nuclear matter that the $A^{2/3}$ dependence could be explained in terms of the optical model with production possible at all nucleons. Imhof (1957) supported this view with experimental evidence over a fairly broad range of meson energies. Belousov et al. (1956) have pointed out that for slow pions the nucleus is almost transparent and that the optical model would then predict $\sigma \propto A$ and the surface model $\sigma \propto A^{2/3}$ independent

TABLE 7.1

Photon energy	140-170	170-200	200-230	230-260	260-290	290-320
$\text{Ni}^{60}(\gamma, \pi^-)\text{Cu}^{60}$ measured σ	2.2	4.2	6.1	5.9	2.6	0.2
$A^{2/3}$ extrapolation from $B^{11}\sigma$ (exp.)	8.6	9.3	9.6	9.6	8.6	5.9
A extrapolation from $B^{11}\sigma$ (exp.)	15.2	16.4	16.9	16.9	15.2	10.4
A extrapolation from $B^{11}\sigma^v$ (calc)	94.0	117.0	104.0	83.0	65.5	52.0

of pion energy. Their results on slow π^0 and π^- mesons are in complete agreement with the "surface production" model.

The Butler-Wilson "surface production" model then has been successful not only in explaining the π^-/π^+ ratios but also in predicting the observed $A^{2/3}$ variation for both fast and slow pions. In the surface model calculations, however, the case in which the recoiling nucleon goes into a bound state in the nucleus, i.e. a reaction of the type (γ, π^-) , had not been considered. All experiments on the A dependence, the present excepted, have involved solely the detection of pions. They have, thus, been unable to discriminate between the cases of the struck nucleon undergoing transitions into discrete or continuum states.

It can be seen from the values of the cross-sections $B^{11}(\gamma, \pi^-)C^{11}$ and $Ni^{60}(\gamma, \pi^-)Cu^{60}$ that the present variation with mass number is less than $A^{2/3}$. In table 7.1 the Ni^{60} measured cross-section is compared with (a) the B^{11} experimental cross-section multiplied by $(60/11)^{2/3}$ (b) multiplied by $60/11$

and (c) the calculated B^{11} cross-section for volume production (Laing and Moorhouse, 1957) multiplied by $60/11$. The Ni^{60} cross-section averaged over the photon energy range 140 to 320 MeV is 40% of that expected by an $A^{2/3}$ - extrapolation of the measured B^{11} cross-section and 25% of the A -extrapolation. Since π^- mesons are produced only at neutrons it would be more correct to consider the variation of the cross-section per neutron with atomic number. The surface model then predicts $\frac{A-Z}{A^{1/3}}$. The effect of this refinement merely increases the extrapolated values by 10% and therefore does not alter the interpretation. The present results are absolutely incompatible with the production of pions throughout the nuclear volume. The fact that the cross-section variation is less than $A^{2/3}$ for all energies of incident photons clearly indicates that this variation is followed for both fast and slow mesons. The results then quite unambiguously support the Butler-Wilson surface production model.

The lack of complete agreement with the $A^{2/3}$ extrapolation is not unexpected. For large Z the

cross-sections for slow π^- production are known to decrease by about 10% from the $A^{2/3}$ dependence because of Coulomb interaction effects (Belousov et al, 1956). Also, Littauer and Walker (1952) have observed that Li^7 and Be^9 have exceptionally large cross-sections for π^- production. B^{11} also, has an extra unpaired neutron and a similar enhancement of π^- production may be expected. It is interesting to note that Popova et al (1959) do not find that the cross-section for slow π^- production is increased for nuclei with excess neutrons. Further, it is not clear to what extent one can define a surface region for nuclei with small A. From scattering experiments the nucleus has a region of uniform density whose radius is $R = r_0 A^{1/3}$, $r_0 = 1.2$ fermis and a region in which the nuclear density drops from 90 to 10 per cent of its previous constant value. The thickness S of this diffuse region is independent of A and $S \approx 2.4f$. For B^{11} the inner region has a radius of 2.7f and the diffuse region extends for a further 2.8f beyond this. Clearly the volume of the diffuse region is very much greater than that of

the core. To define the surface region for π^- production one would have to determine the extent of the diffuse surface region with respect to neutron density. Taking into account the extra unpaired neutron in B^{11} , it may be expected that the surface region is less than that defined by the scattering experiments for other nuclei. It would appear, then, that by considering Coulomb effects in Ni^{60} and the extra unpaired neutron in B^{11} the divergency from the $A^{2/3}$ can be explained.

7.3 The magnitudes of the cross-sections

The one failure of the surface production model was that the calculated cross-sections were about 40% lower than the experimental values for all A. It has already been noted that the calculated values do not include the case in which the struck nucleon goes into a discrete state in the nucleus. It is of interest to determine if reactions of the type (γ, π^-) contribute appreciably to the π^- production cross-section.

For an incident photon energy of 255 MeV the values of the cross-sections $B^{11}(\gamma, \pi^-)C^{11}$ and

$\text{Ni}^{60}(\gamma, \pi^-)\text{Cu}^{60}$ are $3.0 \times 10^{-29} \text{cm}^2$ and $4.4 \times 10^{-29} \text{cm}^2$ respectively. If it is assumed that the Ni^{60} value lies close to the general $A^{2/3}$ dependence and that the B^{11} value has been enhanced, then the extrapolated value for a (γ, π^-) cross-section in carbon will be $1.5 \times 10^{-29} \text{cm}^2$. The B^{11} value is found to be a factor of 2.25 times the $A^{2/3}$ value. It is remarkable that the π^-/π^+ ratios in Li^7 and Be^9 , each also with an extra unpaired neutron, are of the order of 2.25. C^{12} is an even-even nucleus and no enhancement would be expected. It has been observed that the π^-/π^+ ratio for this nucleus is close to unity.

For 255 MeV photons, Steinberger and Bishop (1952) have measured the total cross-section for π^+ production in hydrogen to be $19.0 \times 10^{-29} \text{cm}^2$. This value was obtained by extrapolating linearly differential measurements to small and large angles and integrating. These authors found also that the π^+ production in carbon was about twice as large as production in hydrogen. This leads to a value of $38 \times 10^{-29} \text{cm}^2$ for the total π^+ production cross-

section in carbon for incident photons of energy 255 MeV. Since the π^-/π^+ ratio is close to unity for carbon, a similar value is to be expected for the total π^- production cross-section.

It can now be seen from these derived cross-sections that (γ, π^-) reactions make a 4% contribution to the total π^- production cross-section. This value is on order of magnitude too small to explain the discrepancies between Butler's calculated cross-sections and Littauer and Walker's experimental values. The difference may arise in the selection of the radius of the nuclear core, in which pion production is assumed to be suppressed. It would perhaps be better to assume instead of pion production falling abruptly to zero at the core boundary that there is a continuous decrease across the boundary. The rate of decrease would of course determine the magnitude of the cross-sections. By a suitable choice of this rate agreement could be reached between the calculated and observed cross-sections. In terms of a model, this implies that nucleons in the outer regions of the core can contribute to pion production.

7.4 Reactions of the type (γ, π^-n)

In an attempt to measure the cross-section of the reaction $\text{Cr}^{52}(\gamma, \pi^-)\text{Mn}^{52m}$, an activity with a half-life close to 40 minutes was observed. It was noted (Chapter 5) that there was a variation with energy but due to the preliminary nature of the runs and to the low intensity of the bremsstrahlung beam a complete energy dependence was not obtained. The activity may be due to Mn^{51} (half-life: 44 minutes) produced by the reaction $\text{Cr}^{52}(\gamma, \pi^-n)\text{Mn}^{51}$. Unfortunately Cr^{49} has a half-life of 42 minutes and may be produced by a (γ, n) reaction on Cr^{50} (4.4%) or by a $(\gamma, 3n)$ reaction on Cr^{52} (83.7%). The similarities of these half-lives makes the conclusive identification of the activity very difficult.

The decay curve of the copper activity produced in nickel showed components that were successfully attributed to Cu^{60} (half-life: 24 minutes), Cu^{61} (3.3 hours) and Cu^{62} (10.1 minutes). The contribution of the 3.3 hour component was greater than expected on the basis of a (γ, π^-) reaction in Ni^{62} (1.2%). The expected cross-section was assumed

to the same as that on Ni⁶⁰. The extra yield then may be due to a (γ, π^-n) reaction in Ni⁶² (3.7%). It should be noted however that Sc⁴³ and Sc⁴⁴ have half-lives of 4 hours and that no hold-back carrier for scandium was employed in the chemical separation. It was expected that any scandium produced in the target would either join the carriers of similar elements (e.g. titanium) or would be deposited on the first filter paper. It is possible, although unlikely, that it would be adsorbed on the final precipitate. There is some doubt, therefore, on whether the extra 3 hour activity can be attributed to the reaction Ni⁶² (γ, π^-n) or not.

A reaction of the type (γ, π^-n) is not one in which the recoiling nucleon is emitted from the nucleus. The recoiling nucleon in the basic π^- production reaction is a proton. The neutron, then must be emitted by either direct collision of the recoiling proton with a neutron in the nucleus or by the "evaporation" of a neutron from the excited nucleus formed when the proton shares its energy with the rest of the nucleus.

The yield of a (γ, π^-) reaction relative to a (γ, π^-n) reaction can be determined by irradiating Cu^{63} (69%) the respective product nuclei being Zn^{63} and Zn^{62} . Zn^{63} is a positron emitter of half-life 38 minutes and Zn^{62} has a half-life of 9.3 hours. Similar reactions in Cu^{65} (31%) lead to 250 day Zn^{65} and to stable Zn^{64} respectively. By a chemical separation of zinc, the cross-sections of these reactions on Cu^{63} could be determined.

7.5 Conclusions

The present results strengthen the surface production model of Butler and Wilson. The B^{11} cross-section is in good agreement with the calculated values of Laing and Moorhouse (1957) based on this model. Further, the dependence of the cross-sections on ~~atomic~~ mass number for both fast and slow pions is $A^{2/3}$, as predicted by the surface production model. The small values of the (γ, π^-) cross-sections are a justification of the assumption of Butler that the recoiling nucleon leaves the nucleus. There are suggestions from the present work that reactions of the type (γ, π^-n) may be detectable.

CHAPTER EIGHT REVIEW OF PHOTOSPALLATION STUDIES

A reaction produced by a high energy particle or photon striking a nucleus and causing a number of low mass particles to be emitted from the nucleus is called a spallation reaction. Some of these particles seem to be emitted by the direct interaction of the incident particle and some by evaporation from an excited nucleus. A study of the production rates of the residual nuclei provides information on the processes by which the particle emissions take place. It is also of interest to compare the effects of bombardment by particles and photons upon the yields of the product nuclides.

The yields of spallation reactions induced by high energy particles on middle weight elements have been fairly extensively studied (e.g. Batzel, Miller and Seaborg (1951), 340 MeV protons on copper; Marquez (1952), 400 MeV neutrons on copper; Heiningger and Wiig (1956), 60, 100, 175 and 240 MeV protons on vanadium; and Reasbeck and Wilson (1958), 980 MeV protons on copper. In all these experiments, the residual nuclei resulting from spallation

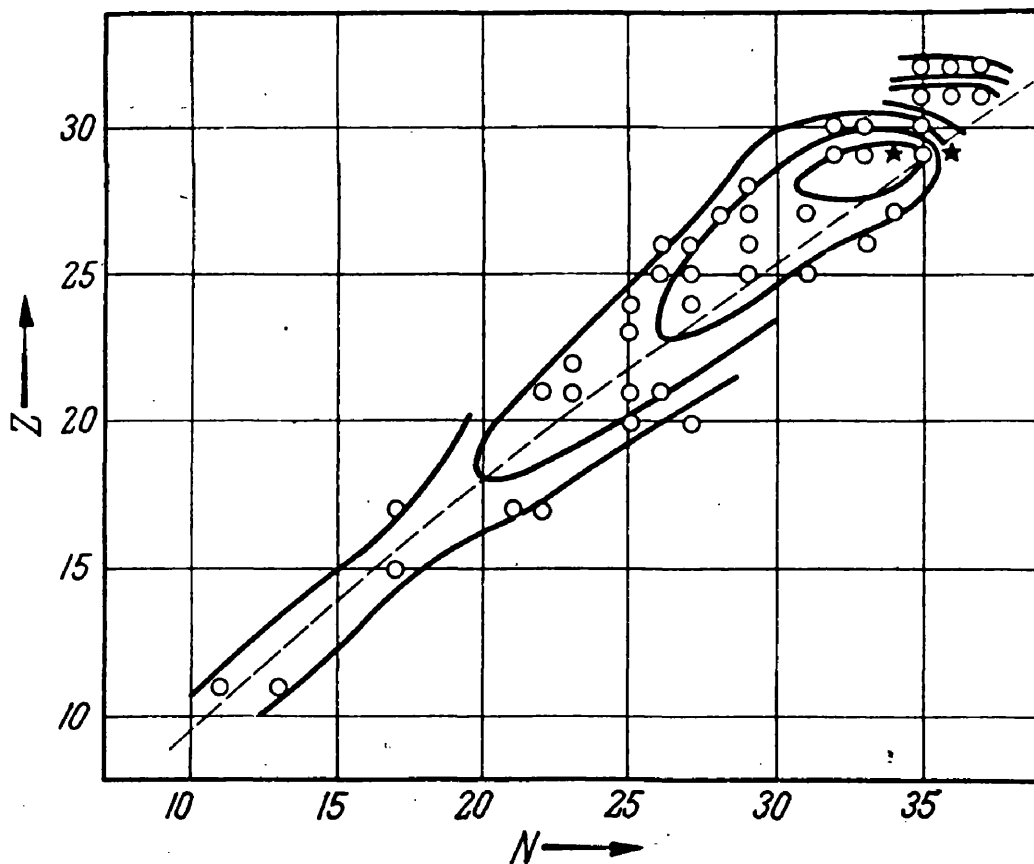
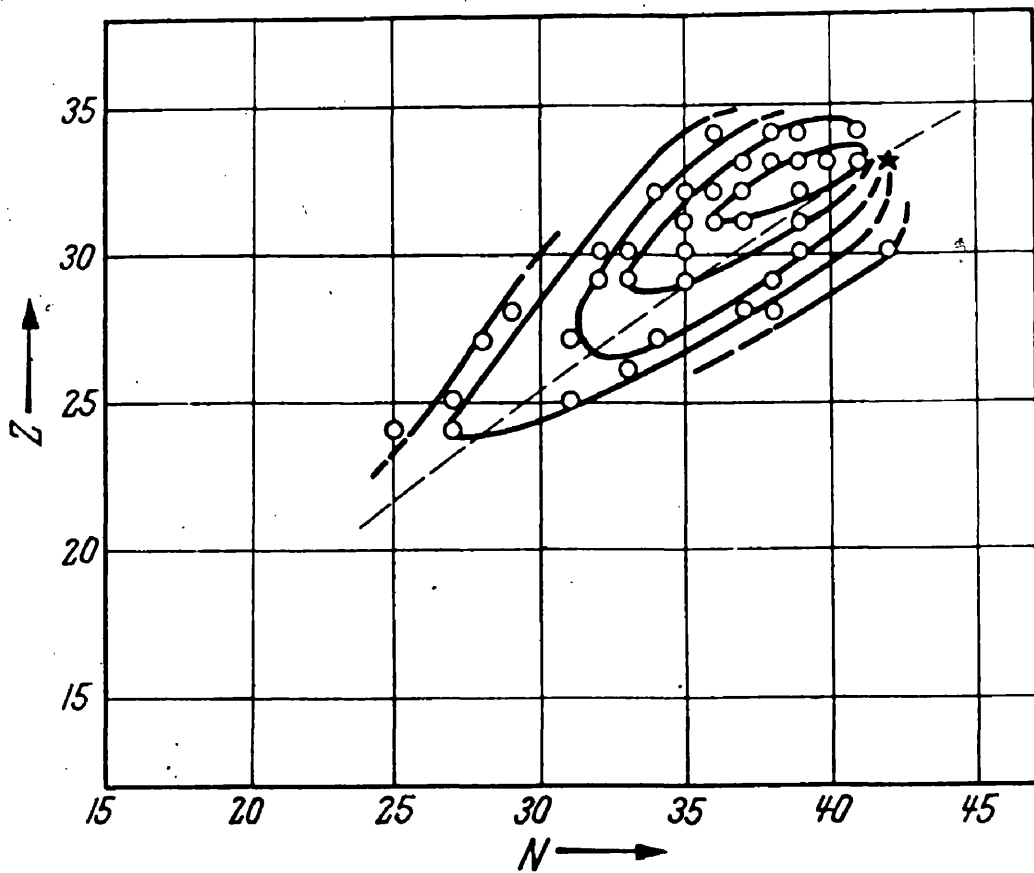


Fig. 5-1 Contour diagrams showing the relative yield of radionuclides plotted in the proton-neutron plane. The circles represent nuclides whose yields were measured; the star indicates the target nucleus (arsenic bombarded by 190 Mev deuterons in the upper, and copper bombarded by 340 Mev protons in the lower figure); the lines connect regions with approximately equal yields, each line representing a factor of ten in yield on an arbitrary scale. [Figure from TEMPLETON: *Ann. Rev. Nucl. Sci.* 2, 93 (1953).]

processes were studied using radiochemical methods.

To make comparisons of the results of the different experiments it has been found convenient to present the yields on a contour map on the Z-N plane, where Z = atomic number and $N = A - Z$, as shown in figure 8.1 (Templeton, 1953). The circles represent those nuclides whose yields were measured and the star indicates the target nucleus. The contour lines connect regions of approximately equal yield and represent a change in yield of a factor of ten, and the dashed line indicates the centre of the stable isotopes of each element. The upper plot shows the yields of nuclides from the bombardment of arsenic with 190 MeV deuterons, Hopkins (1950) and the lower, copper with 340 MeV protons, Batzel Miller and Seaborg (1951).

The experiments exhibit the following general tendencies:

- (a) The highest yields correspond to the emission of three to seven nucleons.
- (b) The magnitude of the yields decreases with

increasing number of ejected nucleons.

(c) The most likely result of spallation is a nuclide near the line of stable isotopes. This clustering of the products along the line of nuclide stability is in disagreement with the expected spread from a random evaporation of neutrons and protons. It can however be explained by the evaporation of deuterons, alpha particles and other small nuclei.

(d) In the region of 100-500 MeV incident particle energy the magnitudes of the yields are a slowly varying function of energy,

(e) As the energy of the incident particles increases so does the number of energetically possible reactions. At higher energies the contour lines become elongated along the line of stable isotopes.

(f) The yield patterns, neglecting those nuclides produced by the emission of one or two nucleons, have very little dependence on the type of bombarding particle.

(g) The yield patterns, i.e. contour diagrams, are qualitatively independent of the target nuclei except

for a regular trend with respect to atomic number. For targets of high atomic number, emitted particles have relatively greater difficulty in penetrating the increased Coulomb barrier. The effect of this is a preferential emission of neutrons to protons with the tendency to produce slightly neutron-deficient isotopes thus displacing the contour lines towards the neutron-deficient side of the line of stability.

The most successful explanation of high energy particle spallation is Serber's (1947) semi-classical picture in which he describes the reactions in terms of the interactions of the incident particles and the individual nucleons of the target nucleus. The mechanism of the reactions can be considered to fall into two separate phases in time. Firstly, a nucleonic cascade is instigated by the collision of the incident particle with one of the nucleons of the target nucleus and the recoiling nucleon either escapes from the nucleus or collides with other nucleons in the nucleus. The products of the secondary collisions either escape or collide with other nucleons, and so on. The cascade continues

until the individual energies of the recoils is insufficient for them to escape from the nucleus. The energy of those nucleons which do not escape is distributed throughout the residual nucleus. The subsequent behaviour of this excited nucleus is described by the evaporation theory of Weisskopf (1937), the excitation energy being dissipated as the kinetic energy of the emitted particles. The distribution of the yields of the reaction product nuclei for particle produced spallation is in general agreement with this model.

Reactions induced by photons of energies up to 70 MeV proceed mainly by a dipole resonance mechanism. The emitted particles result from the evaporation of an excited compound nucleus, although some appear to arise from the direct interaction of the photon and the nucleon subsequently ejected. Photoreactions in this energy region have been studied by several authors e.g. Perlman and Friedlander (1948), Sugarman and Peters (1951), and Schupp and Martin (1954).

At higher energies the only reported photospallation

studies are those of Debs et al. (1955), Sugihara and Halpern (1956) and Wolke and Bonner (1956) on medium weight elements. Their results show the same general trends as those of particle spallation and it has been shown by Debs et al. that the yields can be explained by the Weisskopf evaporation theory. The results differ in that the emission of one or two nucleons is the more likely outcome of "giant resonance" absorption in the low energy region of the bremsstrahlung spectrum.

Debs et al. (1955) bombarded a series of medium weight elements with 320 MeV bremsstrahlung and determined the production rates of the final radionuclides by chemical techniques. The yield patterns seemed to depend more on the properties of the residual nuclei than on those of the struck nuclei of the reactions, suggesting that evaporation is the dominant mechanism. It appeared in a comparison with particle bombardment that the observed yield patterns were to a considerable extent independent of both the nature and the energy of the incident particle. Although the nature of

the initial process could not be postulated from the observed data, the complete reaction was considered to be of the cascade type followed by evaporation from a highly excited nucleus.

Sugihara and Halpern (1956) have re-examined the yields from arsenic for 320 MeV bremsstrahlung and also measured the yields for 140 MeV bremsstrahlung with a view to obtaining excitation curves for the photoproduction of radioactive nuclides. The results at 320 MeV are within a factor of two of those of Debs et al. They suggest that it would be interesting to obtain detailed information about the behaviour of the production cross-sections between 140 and 320 MeV to learn if possible which reactions are associated with free meson production and which are not. Such mechanisms have been suggested by Miller (1951) and Kikuchi (1951), the emission of particles being the result of the production and reabsorption of mesons inside the nucleus. For reactions proceeding in this manner, one may expect a significant rise in the production cross-section above the threshold for

free meson production.

Excitation curves for the production of some radionuclides from the exposure of cobalt to bremsstrahlung beams of maximum energies ranging from 174 to 309 MeV have been determined by Wolke and Bonner (1956). When the yields were plotted against bremsstrahlung peak energy, it was found that (a) photons with energies greater than 174 MeV appear to contribute substantially to the total yield, and (b) the yields curves rise more steeply with increasing energy for increased change in atomic mass, indicating that the "effective photon" energy increases with increasing number of ejected nucleons.

No measurements were reported for energies below 174 MeV.

The work to be described in the following chapters was undertaken to determine the excitation functions of a number of photoreactions in the region of meson production threshold (140 MeV) and to extend previous photospallation results to elements of lower atomic weight. The measurements consist of determinations of the yields of the nuclide F^{18} produced in

- (a) F^{19} , Na^{23} and Al^{27} by bremsstrahlung of peak photon energies ranging from 90 to 240 MeV, and in
(b) Mg^{24} , Si^{28} , P^{31} and S^{32} by bremsstrahlung of 240 MeV peak energy.

The variations of the cross-sections with peak beam energy and with the number of emitted nucleons are determined and the mechanisms of the reactions discussed.

CHAPTER NINE HIGH ENERGY PHOTOSPALLATIONLEADING TO F¹⁸9.1 Experimental Procedure

Hitherto spallation studies have involved the measurement of the activities of the residual nuclei produced in reactions of the type (γ, xN) where x is an integer and N is a nucleon, for a particular target element. This method has a number of disadvantages. It necessitates an accurate radio-chemical separation for every nuclide to be studied, each with its own separation efficiency. Comparisons of the activities of nuclei of different half-lives are very sensitive to fluctuations in beam intensity, while the decay schemes of the various residual nuclei are generally not known to the same degree of accuracy. Wolke and Bonner (1956) have estimated that the errors in their yields due to such inaccuracies vary up to a value of 7%. These difficulties have been overcome in the present work by bombarding a series of stable nuclei and measuring the activity of the same product isotope in each case. In the measurement of the activity

of F^{18} produced in F^{19} , Na^{23} , Mg^{24} , Al^{27} , Si^{28} , P^{31} and S^{32} , the decay scheme of F^{18} is accurately known and no chemical separation is necessary, since there are no nuclei with similar activities in the mass region studied. A further counting error is eliminated by the coincidence detection system employed.

Two series of exposures were made. In the first F^{19} , Na^{23} and Al^{27} were exposed to bremsstrahlung of 90, 120, 150, 180, 210, and 240 MeV peak energy. In the second, a set of target elements of increasing atomic number, F^{19} , Na^{23} , Mg^{24} , Al^{27} , Si^{28} , P^{31} and S^{32} were exposed to bremsstrahlung of peak energy 240 MeV. In each exposure the reaction $C^{12}(\gamma, n)C^{11}$ in carbon was used as a monitor.

The targets consisted of high purity powdered sodium fluoride, sodium peroxide, red phosphorus, silicon and magnesium, four $\frac{1}{16}$ " thick sheets of aluminium, $\frac{1}{8}$ " thick sheet of distrene (C_8H_8) and a cast block of flowers of sulphur. The powders were packed uniformly into thin walled copper boxes of dimensions 1" x 1" x $\frac{1}{4}$ ", the sheets were cut into

1" squares and the sulphur melted and cast in a 1" x 1" x $\frac{1}{4}$ " block. For the first set of measurements a distrene sample, targets of two of the following sodium fluoride, sodium peroxide and aluminium were exposed simultaneously, one behind the other with the target producing the greatest activity at the rear, to the uncollimated bremsstrahlung beam of the Glasgow electron synchrotron at a distance of one metre from the 0.02" diameter internal tungsten target. The peak energy of the beam was varied by 30 MeV intervals from 90 to 240 MeV, and the exposure time varied from thirty minutes to two hours, the longer times generally corresponding to the lower energy beams. For the second series of exposures, targets of sodium fluoride, sodium peroxide, magnesium, silicon, phosphorus and sulphur were exposed in pairs with either a sample of distrene or aluminium (or both) to beams of peak energy 240 MeV, under the same conditions as the first series. The weights of the targets used were about 5 grams each.

After exposure the material was transferred

to other copper boxes with walls thick enough to absorb the 0.65 MeV and the 0.97 MeV positrons from the decay of F^{18} and C^{11} respectively. The positron activities of the C^{11} and F^{18} (half-life:- 111 minutes) in the other targets were measured by counting in coincidence the 0.51 MeV quanta from the positron annihilation.

9.2 Treatment of Data

The measured activities were corrected for background; background rates were measured regularly and found to be constant; for low activities the background was determined immediately before and after the measurement of the desired activity to obtain a more accurate background subtraction. The activities were corrected for decay both during and after irradiation. The value of the F^{18} half-life used in these calculations was 111 minutes.

The activities of the samples were measured at a time when all the short-lived activities produced in them had decayed to negligible proportions. These were an activity of half-life 2 minutes due to O^{15} in the distrene and of O^{15} , 10 minute N^{13} and 20.5 minute

C^{11} in the ...
 and deep ...

Target Element	Most Abundant Isotope	Correction in terms of 1 cm Al. %	Effective Energy of absorbed photon
S	S^{32} : 95%	7.8%	70 MeV
P	P^{31} : 100	7.0 "	70 "
Si	Si^{28} : 92.2	6.8	60
Al	Al^{27} : 100	6.6	50
Mg	Mg^{24} : 78.8	6.4	40
Na	Na^{23} : 100	6.2	30
F	F^{19} : 100	6.0	20
C	C^{12} : 98.9	6.0	20

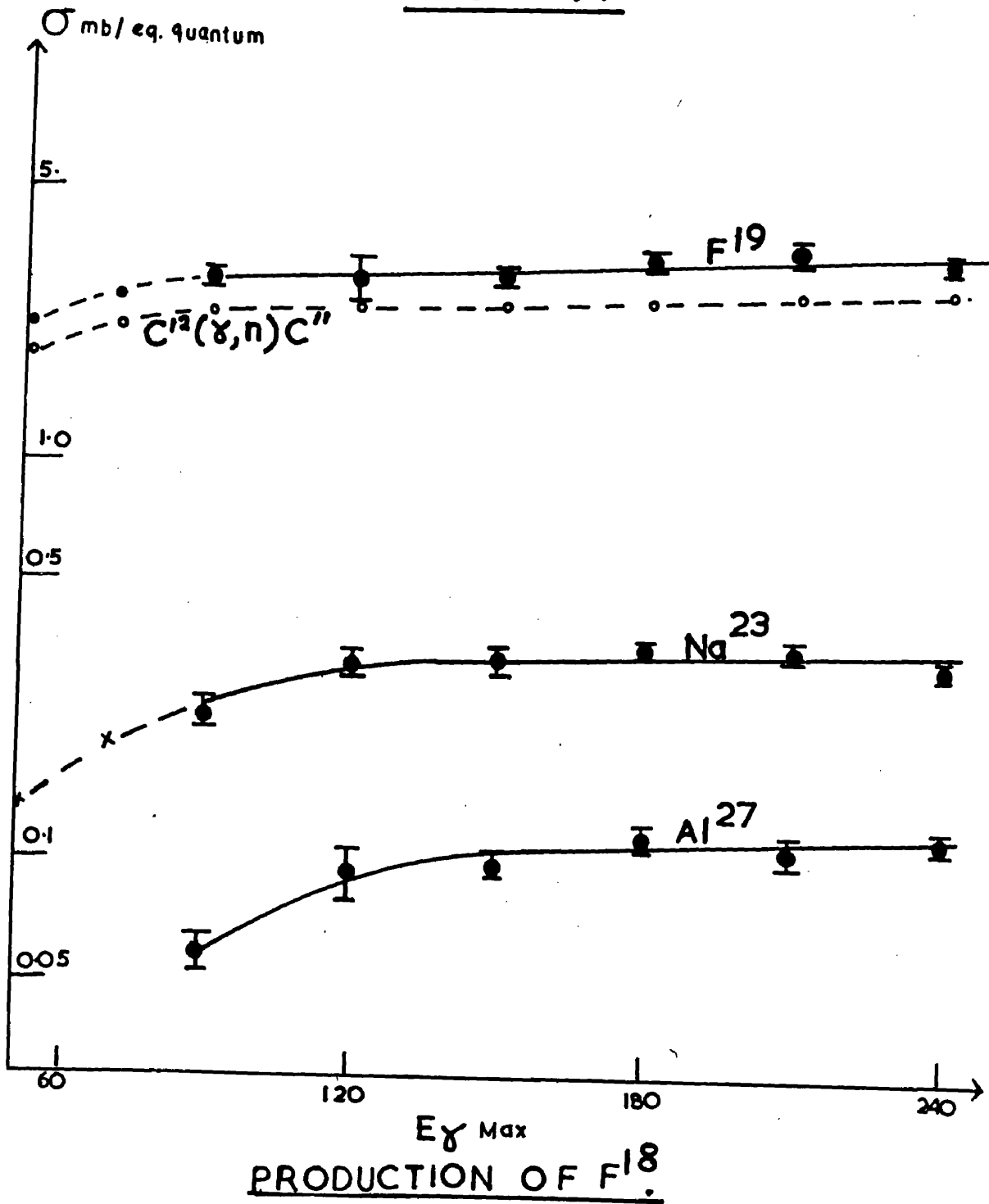
taken to be
 a little ...
 and Martin
 reaction has
 that the cr
 table 3.1,
 are shown
 at which the
 taken are
 of target
 aluminum,

TABLE 9.1

C^{11} in the other targets, due to water impurities and deep spallation; all were small in comparison with the activity of F^{19} . In the case of the sodium peroxide targets, the activities are quite appreciable due to the oxygen content and these targets were not counted until at least two hours after irradiation.

Corrections were made for the absorption of the bremsstrahlung beam in the targets and containers. Where a (γ, n) process was involved the absorption coefficient used was that for a 20 MeV photon since the reaction proceeds predominantly by the interaction of photons of this energy. For the other reactions involved the effective absorption coefficients were taken to be those corresponding to photon energies a little above the estimated thresholds. Schupp and Martin (1954) have shown that the $Ca^{40}(\gamma, 3p3n)Cl^{34}$ reaction has a threshold in the region of 35 MeV and that the cross-section is peaked at 50 MeV. In table 9.1, correction factors in terms of aluminium are shown for the reactions involved; the energy at which the effective absorption coefficients were taken are also listed. The total equivalent thickness of target material was generally of the order of 1 cm aluminium, for which the maximum correction can be

FIGURE 9.1



production of F^{18} from F^{19} , Na^{23} , Mg^{24} , Al^{27} , Si^{28} , P^{31} and S^{32} to the cross-section of the monitoring reaction $C^{12}(\gamma, n)C^{11}$ were obtained on the assumption that the elements considered were 100% abundant in their main isotope. The actual natural abundance of the most abundant isotope is shown in table 9.1; the differences from 100% are low and the errors introduced by such a simplification are, therefore, small.

Finally the results of Barber et al. (1955) for the cross-section of the reaction $C^{12}(\gamma, n)C^{11}$ as a function of maximum bremsstrahlung energy were used to obtain the absolute values for the cross-sections of the reactions studied.

9.3 Results

The variation of the cross-section for the production of F^{18} from F^{19} , Na^{23} and Al^{27} as a function of maximum bremsstrahlung energy from 90 to 240 MeV is shown on figure 9.1. The results of Barber, George and Reagan (1955) for the monitoring reaction $C^{12}(\gamma, n)C^{11}$ are also shown. The values at 50 and 70 MeV for Na^{23} and F^{19} are the work of

Holtzmann and Sugarman (1952) and Perlman and Friedlander (1948), respectively. The present excitation curves are continued through these results by dashes. All cross-sections are in units of 10^{-27} cm^2 per equivalent quantum.

At a peak bremsstrahlung energy of 240 MeV, the cross-sections for the F^{18} reactions originating in the nuclei studied are; F^{19} , 3.5 ± 0.3 ; Na^{23} , 0.33 ± 0.03 ; Mg^{24} , 0.20 ± 0.02 ; Al^{27} , 0.12 ± 0.01 ; Si^{28} , 0.06 ± 0.01 ; P^{31} , 0.08 ± 0.04 ; S^{32} , 0.03 ± 0.01 ; all in units of 10^{-27} cm^2 per equivalent quantum.

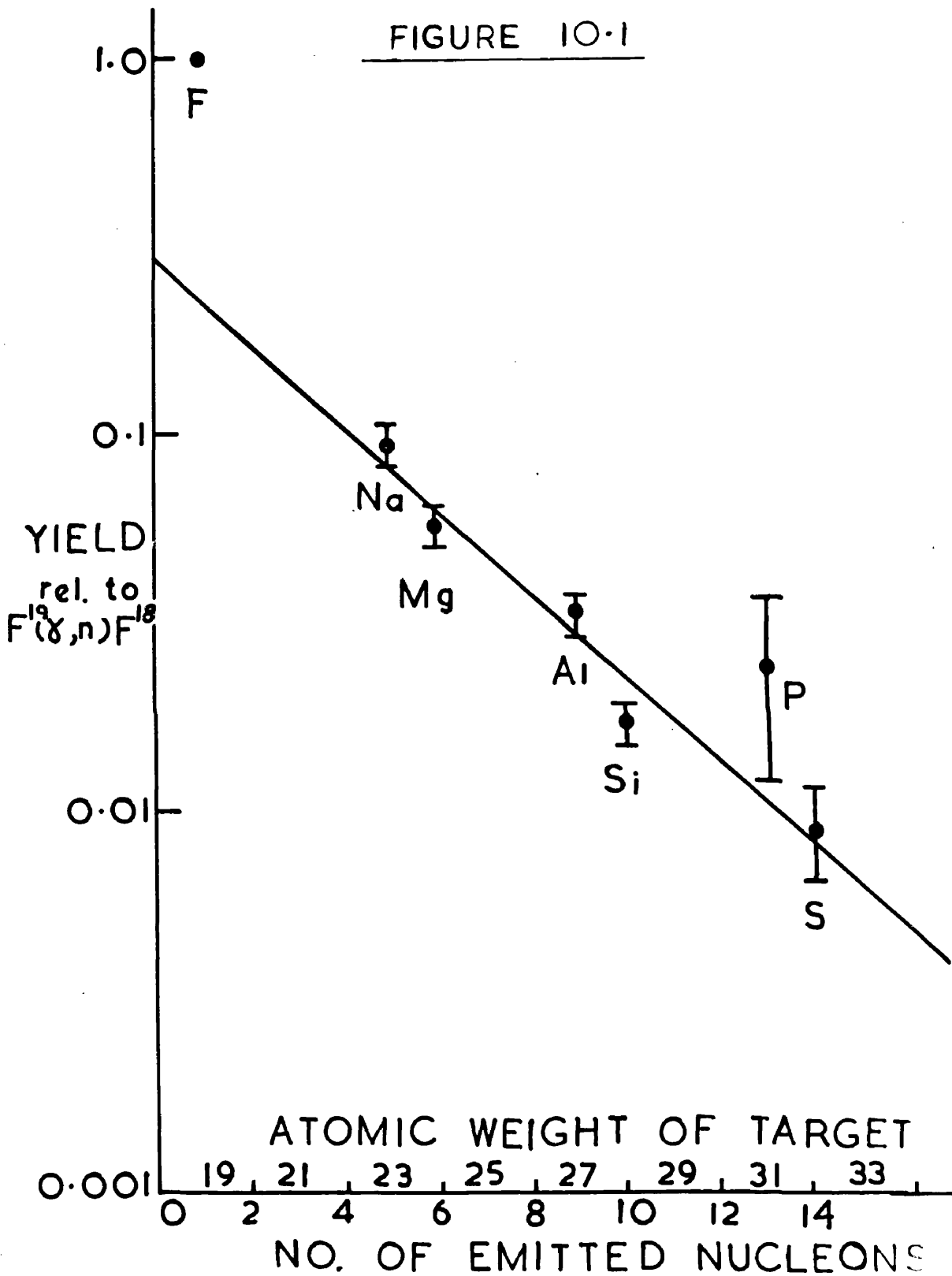
Schupp and Martin (1954) have measured the cross-section for the production of F^{18} from Mg^{24} at an energy of 70 MeV to be $0.17 \times 10^{-27} \text{ cm}^2$ per equivalent quantum, in good agreement with the present value at 90 MeV.

CHAPTER TENPHOTOSPALLATION DISCUSSION

The ratios of the cross-sections for the formation of F^{18} from Na^{23} , Mg^{24} , Al^{27} , Si^{28} , P^{31} and S^{32} to the cross-section for the formation of F^{18} from F^{19} are shown in figure 10.1 plotted against the number of emitted nucleons. It has been assumed that each element is 100% abundant in its most abundant isotope. As would be expected the results indicate that for a given bombarding energy the cross-section for a reaction decreases as the number of emitted particles increases. For processes in which more than one nucleon is emitted the logarithm of the yields relative to the $F^{19}(\gamma,n)F^{18}$ reaction lie, within the present statistics on a straight line of gradient 0.30 ± 0.04 when plotted against the number of emitted nucleons. No attempt was made to draw this line through the point corresponding to the reaction $F^{19}(\gamma,n)F^{18}$, since (γ,n) processes are predominantly produced by the low energy quanta of the bremsstrahlung beam (Barber et al. (1955) and so are not of the cascade type.

As is common to most spallation studies there

FIGURE 10-1



exists a slight ambiguity as to the direct product nucleus of the spallation reaction. The nucleus F^{18} can arise as a direct result of spallation or by the decay of another direct spallation product. For example, direct spallation to F^{18} and to Ne^{18} , Na^{18} etc, i.e. nuclei with the same atomic mass but larger charge than F^{18} , and their subsequent decay to F^{18} by the emission of one, two etc. β^+ particles are possible modes of formation of F^{18} nuclei. Nuclei of the type Ne^{18} , Na^{18} etc. would be expected to have very short half-lives and consequently all the F^{18} nuclei would be produced very shortly after exposure. It has been shown in the work of Debs et al. (1955) that for photon induced spallation, the yield of nuclei of the same mass number decreases rapidly with the distance of these nuclei from the line of stable nuclei on the isotope chart. For F, Ne, Na the masses for maximum nuclear stability are 18.8, 20.9, 23.1 (after Coryell, 1953) so that F^{18} , Ne^{18} , Na^{18} are 0.8, 2.9, 5.1 mass units from the line of nuclear stability. Consequently the direct production of F^{18} nuclei is the predominant mode of formation.

Rudstam (1953) has reported for the spallation of medium weight elements bombarded with protons of energy 187 MeV, a gradient of the order of 0.32 and that the gradient increases with decreasing bombarding energy. Since the present experiment employed a bremsstrahlung beam with a maximum energy of 240 MeV, the mean photon energy will be considerably lower than this. The effective mean energy will depend on the shape of the bremsstrahlung spectrum and of the cross-section curve of the reaction considered. This makes a direct comparison of photon and proton induced spallation difficult. A further difference is the low momentum of a photon compared with a proton of the same energy, suggesting that the Serber (1947) cascade part of the spallation mechanism will be different for photons and protons.

It should be noted that since the present residual nucleus F^{18} is 0.8 mass units lighter than the stable valley, the F^{18} yield will lie approximately on the yield curve described by Debs et al. (1955).

The present gradient should then correspond to the gradient of the ridge of the yield surface on the

neutron-proton plane for low atomic weight elements. Owing to the paucity of other photo-yields along this ridge, the gradient cannot be determined from the results of other authors, although it does appear to be of the same order of magnitude as the present value.

The prong distribution of photo-stars in emulsions is a measure of the number of particles emitted in the reactions, Kikuchi (1951), Peterson and Roos (1957) and others have found the relative number of events with respect to prong number in emulsions exposed to 300 MeV bremsstrahlung. However for an event with six prongs, say, the total number of emitted nucleons is doubtful. These six prongs are known to be charged particles, but may be protons, deuterons, alpha particles etc; an unknown number of neutrons may also have been emitted. A further complication is that radioactive techniques fail to observe the stable products; an emulsion, on the other hand, records the emission of charged particles only. It is, therefore, not possible to compare the yields of radio-nuclides with the number

of stars in emulsions.

The excitation curves on figure 9.1 show the expected rise in cross-section for increase in bremsstrahlung peak energy. The present results are quite consistent with previous low energy measurements as can be seen by the extrapolated curves.

The yield curve of F^{18} from F^{19} displays the same form as that of the monitoring reaction $C^{12}(\gamma,n)C^{11}$. Since these two reactions are both (γ,n) reactions the only difference in the cross-sections to be expected would be that for the increase in atomic number. The $F^{19}(\gamma,n)F^{18}$ cross-section is greater than the $C^{12}(\gamma,n)C^{11}$ cross-section by a constant factor of 1.2. Since the excitation curve remains fairly flat above 100 MeV, the higher energy quanta in the bremsstrahlung beam contribute little to the yield. The reaction proceeds predominantly by the "giant resonance" photons i.e. of energy in the region of 20 MeV.

The excitation curve for F^{18} production from Na^{23} shows a more rapid rise at the lower energies

PRODUCTION CROSS SECTION (approx.)

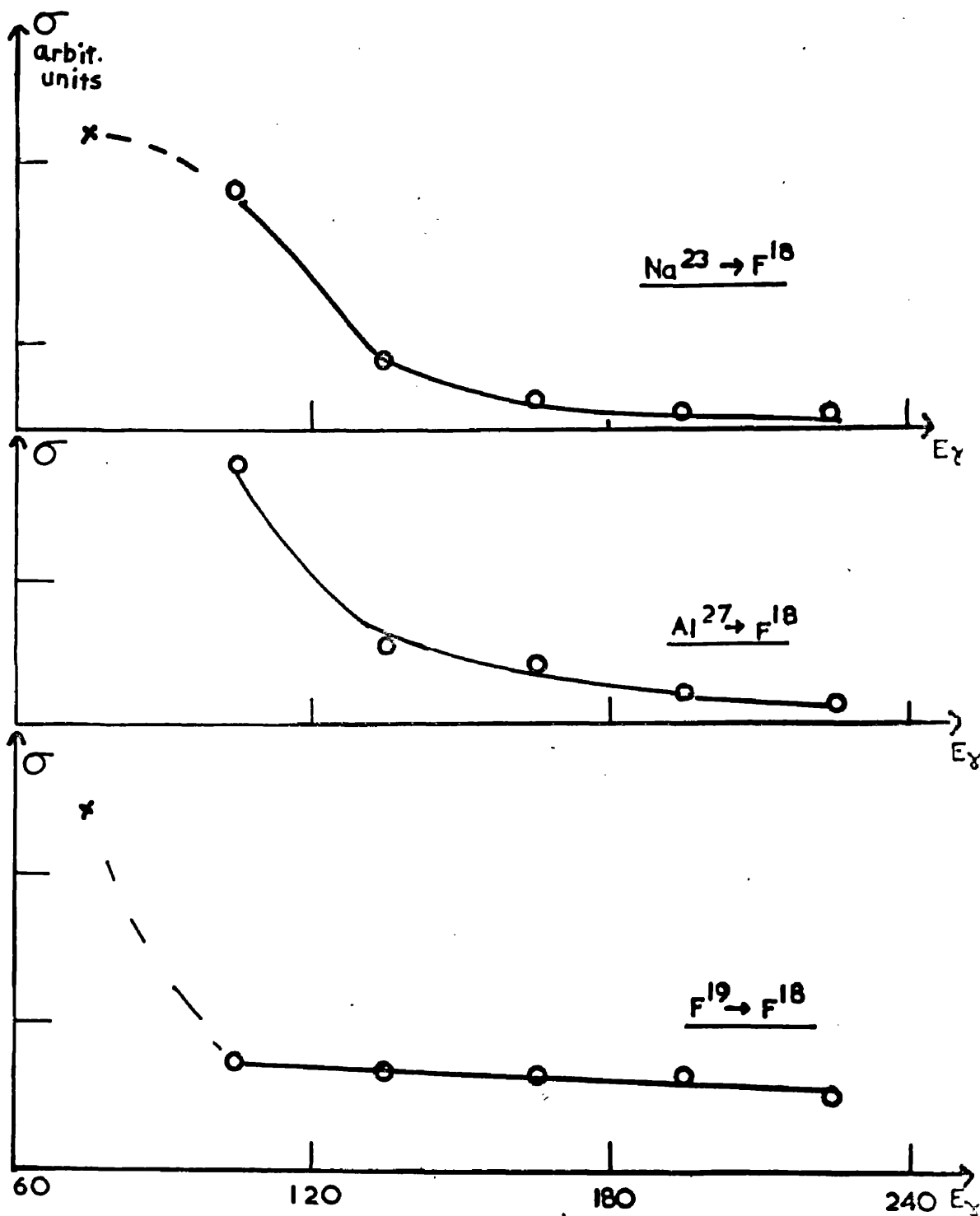


FIGURE 10-2

studied and a flat section appearing at a higher energy (150 MeV) than the F^{19} curve. F^{18} is then produced from Na^{23} predominantly by quanta of energy less than 150 MeV. The Al^{27} curve shows the same trend but there is a more rapid increase in yield at lower energies and a lesser tendency to level off at higher energies.

In figure 10.2, the difference in yields for each increase of 30 MeV in the peak bremsstrahlung energy is shown as a function of mean energy of the interval. The curves which have been drawn through these points, can be taken to represent the cross-section of the reactions studied for photons of energy corresponding to the mean energy of the interval. These curves will then show the variation of cross-section with incident photon energy. It is indicated from the shape of the curves that these reactions proceed by the absorption of the lower energy quanta in the bremsstrahlung beam. By comparing the yields at 240 and 120 MeV peak bremsstrahlung energy it appears that quanta of energy between 120 and 240 MeV contribute of the order of 12, 12, and 21% to the

F^{18} production cross-sections from F^{19} , Na^{23} and Al^{27} .

No abrupt change in the shapes of the curves of figures 9.1 and 10.2 can be observed as the photon energy is increased above the photomeson production threshold (140 MeV). This suggests that the "free-meson" effect is not a predominant mechanism of photospallation. Such effects have previously been suggested by Bruno and Depken (1952) and Wilson (1952) to explain photodisintegration. Bruno and Depken postulated that a meson emitted by one nucleon, absorbs the photon and is then itself absorbed by a neighbouring nucleon. Wilson on the other hand, described a mechanism whereby a meson is created by the absorption of a photon by a nucleon and the subsequent reabsorption of the meson by a two nucleon system consisting of the original nucleon and its nearest neighbour. These two nucleons could then produce a nucleonic cascade and particle evaporation of the Serber-Weisskopf type. These meson effects might be expected to significantly increase the spallation yields above meson production threshold. Although a possible mechanism, the present work shows that it

does not appear to be the main one.

Debs et al. (1955) have shown that photospallation results exhibit the same characteristics as those of particle spallation and conclude that the mechanisms of the reactions are of the same type regardless of the type of incident beam. However, since the momentum of a photon is low compared to that of a particle, it is to be expected that the initial absorption of the photons and particles in the cascade part of the spallation mechanism will be different. A possible mode of absorption is given by the quasi-deuteron model in which the photon is considered as interacting with a two nucleon pair in the nucleus, these two energetic nucleons then initiating a Serber cascade. The absorption mechanism is then the same as that responsible for the photodisintegration of a free deuteron. In a photospallation reaction described by "quasi-deuteron absorption" and "cascade-evaporation" emission of particles, the yields would follow the Serber-Weisskopf distribution. The excitation curves would be expected to have a similar form as the absorption curves, i.e. having a maximum

at low energies and a long tail at higher energies. The position of the maximum would depend on the number of nucleons emitted, higher energy photons producing greater nuclear excitation and consequently a greater number of emitted nucleons. Since the emitted particles may consist of combinations of nucleons, then the maximum would be fairly broad corresponding to the different individual thresholds and maxima of the possible reactions.

The present photospallation studies give the cross-sections for reactions not hitherto studied. The general features of the values are similar to previous spallation studies. The variation of the cross-sections with incident photon energy shows that the production rates are fairly constant for photon energies greater than 100 MeV. This fact was assumed in the subtraction of the activity below meson threshold from that above in the (γ , π^-) investigations, which constituted the main part of this thesis.

REFERENCES

- Ajzenberg-Selave, T., and Lauritsen, T., 1959, Nuc. Phys., 11, 1. (the properties of the isotopes; no reference given in text).
- Baldin, A.M., and Lebedev, A.I., 1958, J.E.T.P. 6(33), 940.
- Barber, W.C., George, W.D., and Reagan, D.D., 1955, P.R., 98, 73.
- Batzel, R.E., Miller, D.R., and Seaborg, G.T., 1951, P.R. 84, 671.
- Belousov, A.S., 1956, C.E.R.N. Symposium, II, 288.
Belousov, A.S., Rusakov, S.V., Tamm, E.I., 1959, J.E.T.P. 35, 247.
- Drueckner, K.A., Serber, R., and Watson, K.M., 1951, P.R., 84, 258.
- Bruno, B., and Depken, S., P.R., 86, 1054.
- Butler, S.T., 1952, P.R., 87, 1117.
- Coryell, C.D., 1953, Ann. Rev. Nuc. Sci., 2, 305.
- Debs, R.J., Eisinger, J.T., Fairhall, A.W., Halpern, I., Richter, H.G., 1955, P.R., 97, 1325.
- Francis, N.C., and Watson, K.M., 1953, P.R., 89, 328.
- George, E.P., 1956, Proc. Phys. Soc. A, 69, 110.
- Heininger, C.G., and Wiig, E.O., 1956, P.R., 101, 1074.
- Hogg, W.R., 1960, Private Communication.

- Hogg, W.R., and Sinclair, D., 1956, Phil. Mag., 1,
466.
- Holtzman, R.B., and Sugarman, N., 1952, P.R., 87,
633.
- Hopkins, H.H., 1950, P.R., 77, 717.
- Hughes, I.S., and March, P.V., 1958, Proc. Phys.
Soc., 72, 259.
- Hummel, J.P., and Dyal, P., 1959, Bull. Am. Phys.
Soc., Ser. 2, 4, 321.
- Imhof, W., Knapp, E.A., Easterday, H., Perez-Mendez, V.,
1957, P.R., 108, 1040.
- Kikuchi, S., 1951, P.R., 81, 1060.
- Laing, E.W., and Moorhouse, R.G., 1957, Proc. Phys.
Soc. B, 70, 629.
- Lax, M., and Feshbach, H., 1951, P.R., 81, 189.
- Littauer, R.M., and Walker, D., 1952, P.R., 86, 838.
- Marquez, L., 1952, P.R., 88, 225.
- Miller, R.D., 1951, P.R., 82, 225.
- Mozley, R.F., 1950, P.R., 80, 493.
- Perlman, M.L., and Friedlander, G., 1948, P.R., 74,
442.
- Peterson, V.Z., and Roos, C.E., 1957, P.R., 105, 1620.

- Popova, V.M., Semashko, N.G., and Yagudina, R.F.,
1959, J.E.T.P., 2(36), 965.
- Reasbeck, P., and Warren, J.E., 1958, J. Inorg. Nucl.
Chem., 7, 343.
- Rosengren, J.W., and Dudley, J.M., 1953, P.R., 89,
603.
- Rudstam, S.G., 1955, Phil. Mag., 46, 344.
- Schupp, F.D., and Martin, D.S., 1954, P.R., 94, 80.
- Serber, R., 1947, P.R., 72, 1114.
- Steinberger, J., and Bishop, A.S., 1952, P.R., 86,
171.
- Sugarman, N., and Peters, R., 1951, P.R., 81, 951.
- Sugihara, T.T., and Halpern, I., 1956, P.R., 101,
1768.
- Templeton, D.H., 1953, Ann. Rev. Nuc. Sci., 2, 93.
- Weisskopf, V.F., 1937, P.R., 52, 295.
- Williams, W.S.C., Crowe, K.M., and Friedman, R.M.,
1957, P.R., 105, 1840.
- Wilson, R.R., 1952, P.R., 86, 125.
- Wolke, R.L., and Bonner, N.A., 1956, P.R., 102, 530.

PUBLICATIONS

1. "High Energy Photospallation leading to F^{18} "
by Walker T. G., and Morton, W. T.,
Proc. Phys. Soc. 75, 4, 1960.
2. "The Photoproduction Reaction $^{60}\text{Ni}(\gamma, -)^{60}\text{Cu}$ "
by March, P. V., and Walker, T.G.;
accepted for publication by Proc.Phys. Soc.
3. "Hammer Tracks from the Photodisintegration of
Light Emulsion Nuclei"
by Morton, W.T., and Walker, T.G.;
accepted for publication by Phil.Mag.
4. " $(\gamma, p + \alpha)$ Reactions in C^{12} , N^{14} and O^{16} "
by Morton, W.T. and Walker, T.G.;
submitted for publication to Phil.Mag.

APPENDIX AHammer Tracks from the Photodisintegration
of Light Emulsion Nuclei.

By W.T. Morton and T.G. Walker

(Department of Natural Philosophy, University
of Glasgow).

If Li^8 or B^8 is produced in a nuclear disintegration it will decay at rest into two alpha particles through an excited state of Be^8 , and so produce a characteristic T shaped track. These are usually referred to as "hammer tracks" (Occhialini and Powell (1947), Alvarez 1950)). Events of this type in which the initial disintegration was produced by a particle have been investigated by a number of workers (for example, Titterton (1951)). In the present investigation a search has been made for hammer tracks originating in the photodisintegration of the light nuclei (carbon, nitrogen and oxygen) of nuclear research emulsions.

Ilford C.2. nuclear research emulsions, 400 microns in thickness, were exposed perpendicular to a bremsstrahlung beam of maximum energy 120 MeV from

the Glasgow electron synchrotron. The emulsions were scanned for nuclear disintegrations in which more than two charged particles were emitted. 4,300 events of this type were examined and eight hammer tracks identified. A small number of the three prong events could have been due to the emission of a Li^8 or B^8 particle from a heavy nucleus of the emulsion (silver or bromine) for which no other charged particle was emitted. These events might be confused with a low energy 3α photodisintegration of C^{12} and so were neglected. In each of the accepted hammer track events the initial disintegration had also produced a singly charged or doubly charged particle of energy less than 5 MeV, and it is considered unlikely that these would be emitted simultaneously with a hammer fragment from a heavy nucleus of the emulsion. Hence it seems reasonable to assume that all of the hammer tracks accepted originated in the light nuclei of the emulsion. In the investigation of hammer tracks emitted in reactions induced by neutrons with an energy of 150 MeV, Titterton (loc. cit.) reached a

similar conclusion. It would be expected that the probability of emission of a hammer fragment from silver or bromine would decrease with energy of the incident particle.

If a B^8 particle was emitted from a carbon nucleus, by the conservation of charge, a singly charged particle would also be emitted. Hence, although the B^8 would be recorded as a three prong event, its true nature would be indicated by the sharp change in grain density and possibly also in direction at the position of the initial disintegration. No events of this type were found. This result is in agreement with Titterton who found that the probability of a hammer track resulting from Li^8 is higher than that for B^8 . In the remainder of this communication all hammer tracks will be assumed to be due to Li^8 .

No events were observed which could be assigned to Li^9 , which decays into Be^{*9} followed by a decay at rest into a neutron and two alpha particles (Fry (1953)). In this case the two alpha particles would not be collinear.

The energies of the Li^8 tracks were found to be 2.2, 3.2, 3.2, 5.1, 6.5, 8.3, 10.5 and 14.5 MeV. Three of the events in which the Li^8 particle originated had three prongs, one of which was singly and the other doubly charged. Hence by charge conservation these events are produced by the reaction $\text{C}^{12}(\gamma, \text{He}^3\text{p})\text{Li}^8$ with a Q value of 41.2 MeV, or by $\text{C}^{13}(\gamma, \alpha\text{p})\text{Li}^8$ (Q=27.6 MeV). The remaining events had four prongs, three of which were due to singly charged particles. These events must also have originated in a carbon nucleus of the emulsion. Since it was not possible to differentiate between protons and deuterons these events were produced either by the reaction $\text{C}^{12}(\gamma, 3\text{p})\text{Li}^8$ with a Q value of 50.9 MeV or the reaction $\text{C}^{12}(\gamma, 2\text{pd})\text{Li}^8$ with a Q value of 48.7 MeV.

To obtain the incident γ -ray flux the three prong events were analysed, using the criteria of Goward and Wilkins (1952), for events produced by the photodisintegration of C^{12} into three alpha particles. Using the cross section given by these authors for that reaction the cross section for the photoproduction of Li^8 from C^{12} averaged over γ -ray

energies between 50 MeV and 120 MeV was found to be
 $(4.9 \pm 2.0) \times 10^{-30} \text{ cm}^2$.

Acknowledgments

The authors wish to thank Dr. P. V. March for useful discussions and Dr. W. McFarlane for operating the synchrotron. One of us (T.G.W.) wishes to thank the Department of Scientific and Industrial Research for a maintenance grant.

References

- Alvarez, L. W., 1950, Phys. Rev., 80, 519.
Fry, W. F., 1953, Phys. Rev., 89, 325.
Goward, E. K., and Wilkins, J. J., 1952, Proc. Phys. Soc., A65, 671.
Occhialini, G.P.S., and Powell, C.F., 1947, Nature Lond., 159, 93.
Titterton, E. W., 1951, Phil. Mag., 42, 113.

APPENDIX B($\gamma, p + \alpha$) Reactions In C^{12} , N^{14} and O^{16}

By W. T. Morton and T. G. Walker

(Department of Natural Philosophy, University
of Glasgow).ABSTRACT

By irradiating normal and water loaded nuclear research emulsions with a bremsstrahlung beam of peak energy 120 MeV, the cross sections for the reactions $C^{12}(\gamma, p \alpha)Li^7$, $N^{14}(\gamma, p \alpha)Be^9$ and $O^{16}(\gamma, p \alpha)B^{11}$ were found to be 1.33, 0.38 and 0.13 MeV mb. The results are compared with those of previous workers.

§ 1. INTRODUCTION

The constituents of a nuclear research emulsion can be divided into two groups; the heavy nuclei (silver and bromine) and the light nuclei (carbon, nitrogen and oxygen). To identify a particular photodisintegration process and the energy of the incident γ ray all the reaction products must be observed and have sufficient length to make possible accurate measurements of energy and angle. The short length of a recoil from a heavy nucleus disintegration limits the emulsion technique to the light nuclei of the emulsion.

Among the reactions suitable for study is the photodisintegration of carbon, nitrogen and oxygen into an alpha particle, a proton and a recoil. This reaction has been studied previously by Livesey (1956b) and Maikov (1958). These authors disagree on the relative frequency with which the $(\gamma, p + \alpha)$ reaction occurs in carbon, nitrogen and oxygen. In the present experiment an attempt has been made to investigate this difference by increasing the proportion of oxygen in a nuclear research emulsion.

The Q values for the reactions $C^{12}(\gamma, p \alpha) Li^7$, $N^{14}(\gamma, p \alpha) Be^9$ and $O^{16}(\gamma, p \alpha) B^{11}$ are 24.6, 18.2 and 23.1 MeV. Because of the high Q values it is necessary to use γ rays of moderately high energy to study these processes. There is no advantage in using γ rays of energy above about 120 MeV, since these would tend to produce a more complete disintegration of the light nucleus.

§ 2 EXPOSURE AND IDENTIFICATION OF EVENTS

Ilford C2 nuclear research emulsions 400 microns in thickness were exposed perpendicular to a bremsstrahlung beam with a maximum photon energy of 120 MeV from the Glasgow electron synchrotron a similar nuclear emulsion in which the thickness was increased by 156 microns by soaking it in distilled water was exposed in the same position.

The emulsions were searched for 3 prong events using a microscope with a magnification of X270. Events were considered only if all the emitted particles stopped within the emulsion. If visual inspection of an event indicated that it may balance momentum the length and angles of its prongs were measured under a magnification of X1350. Because of the difficulty in obtaining accurate measurements on short tracks all events in which one of the prongs had a length less than $1\frac{1}{2}$ microns were eliminated. The measured events were chiefly of two types. One group consisted of events in which none of the emitted particles was singly charged and the other group of events in which one of the prongs resulted from a singly charged particle.

A system of units was used in which the momentum of a 1 MeV proton was taken as 1 mass unit of momentum. Events in which one of the prongs was singly charged were analysed by first assuming the singly charged particle to be a proton and considering in turn each of the other particles to be an alpha particle. Using this assumption the resultant momentum of the proton-alpha pair was calculated perpendicular to the direction of the third particle. The event was rejected if the lack of balance perpendicular to the third particle direction was greater than ^{one} momentum unit. In each case, for which a possible balance was obtained, the length of the particle assumed to be

NAME

HUNWELL

B7203

No

PHOTOGRAPHIC GROUP

UNCLASSIFIED

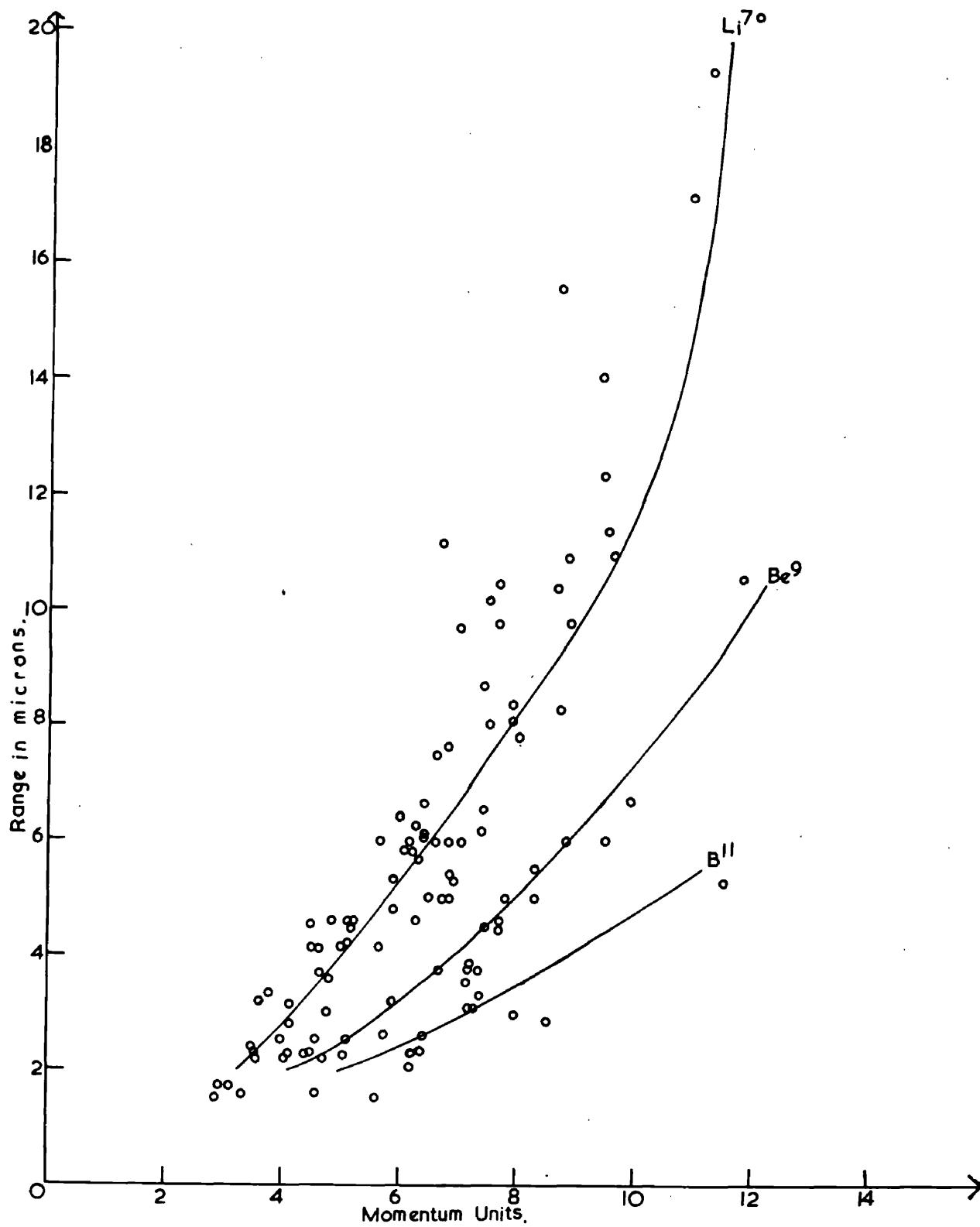


Fig. 1 Comparison of experimental points with theoretical curves for Li^7 , Be^9 and B^{11} ions.

an alpha particle was greater than that of the third particle. In the subsequent analysis the shortest track was assumed to be due to the recoil. Since it was not possible to distinguish protons and deuterons by grain counting, the resultant momentum was again calculated perpendicular to the recoil direction assuming that the singly charged particle was a deuteron. If the lack of balance was smaller, the event was eliminated. In this way 20% of the events, which would otherwise have been accepted, were rejected. The 111 events which remained were assumed to be genuine (γ , p + α) events in light emulsion nuclei.

The resultant momentum of the alpha particle and proton was calculated in the direction of the recoil and plotted against the range of the recoil (figure B1) for the accepted events which occurred in the normal emulsions. Also shown on figure 1 are the theoretical range momentum curves of Livesey (1956b) for Li^7 , Be^9 and B^{11} particles. A grouping of events was observed close to the Li^7 curve.

Three prong events, in which none of the prongs was due to singly charged particles, were analysed using the criteria of Goward and Wilkins (1953) for photodisintegrations of C^{12} into three alpha particles. Using these results for normalization absolute values were obtained for the cross sections of the

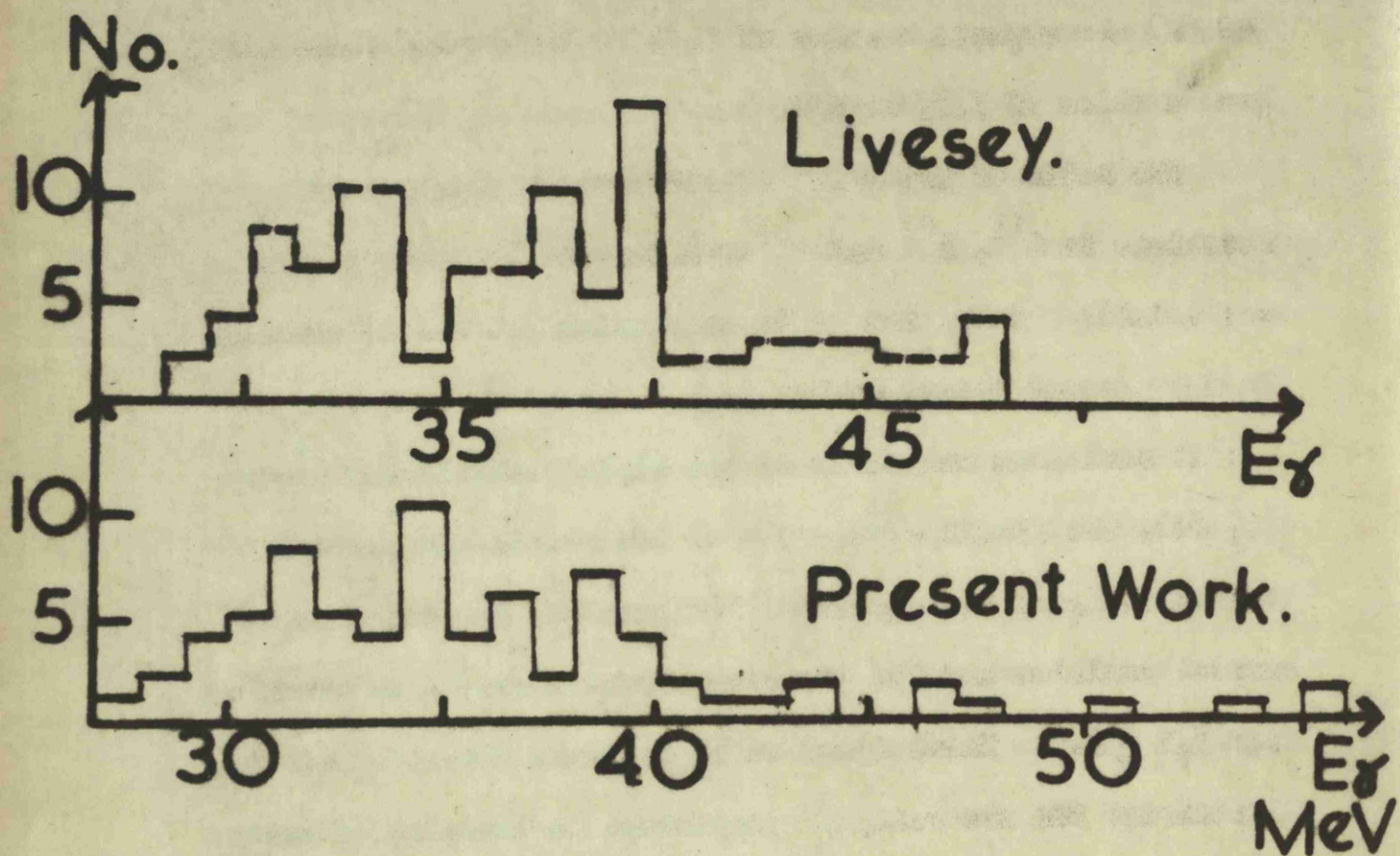


Fig. B2. $C^{12}(\gamma, p + \alpha) Li^7$.

reaction $(\gamma, p + \alpha)$ in the nuclei C^{12} , N^{14} and O^{16} .

§3 RESULTS AND DISCUSSION

The integrated cross section for the reaction $C^{12}(\gamma, p \alpha) Li^7$ from 25 to 40 MeV obtained in the present study was 1.2 mb MeV, in satisfactory agreement with Livesey (1956b) who reports a value of 1.33 mb MeV Maikov (loc. cit.) gave a value of 3.85 mb MeV.

The ratio of the cross section for the $(\gamma, p + \alpha)$ reactions in C^{12} , N^{15} and O^{16} obtained by Livesey (1956b) was 1:0.28:0.05, and by Maikov (loc. cit.) was 1:0.36:0.63.

In the present investigation, using the events found in the normal emulsions and the range energy relations of Livesey (1956a), the result obtained is 1:0.28:0.10. In the water loaded emulsion the oxygen content was 2.4 times that of a normal emulsion and the increase in the $O^{16}(\gamma, p \alpha) B^{11}$ events was 3.7 ± 2.0 . There appeared to be no significant loss in efficiency for observing proton prongs in the water loaded emulsion as the cross section for the $C^{12}(\gamma, p \alpha) Li^7$ reaction in the normal emulsion and in the water loaded emulsion were found to be identical.

In figure B2 the solid histogram shows the cross section for the reaction $C^{12}(\gamma, p \alpha) Li^7$ as a function of γ ray energy

in the present experiment, the dotted curve gives the results of Livesey (1956b).

It is not possible to obtain conclusive results as to which particle is emitted first in the $(\gamma, p + \alpha)$ reaction, because of the limited energy resolution of the technique and the large number of levels through which an intermediate nucleus could decay. In 65% of the events originating in C^{12} , and in 92% of the O^{16} events, the alpha particle has a higher energy than both the proton and the recoiling nucleus. This suggests that the alpha particle is emitted first and the subsequent disintegration takes place through an excited state of Be^8 in the case of the $C^{12}(\gamma, p \alpha) Li^7$ reaction.

ACKNOWLEDGMENTS

The authors would like to thank Miss M. Thompson for assistance with the microscope work, Dr. P. V. March for useful discussions, and Dr. W. McFarlane for operating the synchrotron. One of us (T.G.W.) wishes to thank the Department of Scientific and Industrial Research for a Maintenance grant.

REFERENCES

Goward, E. K. and Wilkins, J. J., 1953, Proc.Roy.Soc., A,217,357.

Livesey, D. L., 1956,a, Can.J.Phys. 34,203.

Livesey, D. L., 1956,b, Can.J.Phys. 34,216.

Maikov, 1958, J.E.T.P. 34,973.